ABSTRACT

ATAR, JESSICA NICOLE. Contrasting estuarine and coastal organic matter dynamics from varying climatic regions. (Under the direction of Dr. Christopher Osburn).

The purpose of this study was to determine differences in dissolved and particulate organic matter (DOM and POM) dynamics among the coastal waters of five regions: the lower Outer Banks, NC (NC); Charleston Harbor, SC (SC); Corpus Christi Bay, TX (TX); Florida Keys, FL (FL); and Kahana Bay, HI (HI) through quantitative and qualitative measurements. The studied sites, NC, SC, TX, FL, and HI, are located along a climatic gradient including humid subtropical, humid subtropical, humid subtropical, tropical savanna, and tropical rainforest climates, respectively, based on the Köppen climate classification system. The transport of DOM and POM through freshwater and estuarine systems includes poorly understood transformation processes occurring in these transitional ecosystems prior to reaching the coastal ocean. Because organic carbon (OC) constitutes a large fraction of the total organic matter pool, the study of DOM and POM transformations is important because of their contributions to the global carbon cycle. The overall objective of this research was to examine if the Köppen climate classifications influenced the quantity and quality of DOM and POM from coastal waters to the coastal ocean. Quantity was measured using dissolved and particulate organic carbon (DOC and POC) concentrations, while quality was assessed through absorbance and fluorescence measurements of chromophoric dissolved organic matter (CDOM) and base extracted particulate organic matter (BEPOM), stable carbon isotopes of DOM and POM, and bulk elemental ratios for the POM size fraction. Additionally, statistical modeling was performed on the dataset using Parallel Factor Analysis (PARAFAC) and Principal Component Analysis (PCA). The major finding from this research was that the Köppen climate classifications did not directly affect

the quantity or quality of organic matter in the estuarine systems studied. Instead local weather factors associated with the sampling location, seasonal time, and local conditions (e.g., precipitation, vegetation, freshwater inputs, and proximity to OC source) influenced the organic matter quantity and quality within each region, and were most evident in POM quality. Another finding from this study was that DOM quantity was variable, whereas POM quantity was similar among the five sites. However, abundances of DOM and POM did not seem to be influenced by the regional Köppen climate classifications. Lastly, the DOM quality was similar in all regions regardless of climate classifications. Similarities in DOM quality were observed in PARAFAC component distributions with relative abundances of the same components across all regions, along with fewer significant differences observed in the qualitative measurements (e.g., optical measurements and stable carbon isotope values). By contrast, POM showed greater variability in quality across regions, reflected in the PARAFAC component distributions, the range in stable carbon isotope values, and bulk elemental ratios. Overall, the results of this research indicated that local weather factors exerted major control on organic matter dynamics in the five region's coastal waters, which translated into estuaries being conduits for DOM and biogeochemical reactors for POM across these interfaces between terrestrial and marine ecosystems.

Contrasting estuarine and coastal organic matter dynamics from varying climatic regions

by
Jessica Atar

A thesis submitted to the Graduate Faculty of
North Carolina State University
in partial fulfillment of the
requirements for the degree of
Master of Sciences

Marine, Earth, and Atmospheric Science

Raleigh, North Carolina

2017

APPROVED BY:

_____	_____
Dr. Christopher Osburn Committee Chair	Dr. David DeMaster

_____
Dr. Karen McNeal

DEDICATION

To my family who has supported me through every step of the way and to my good friends that have stayed by my side through all the obstacles.

BIOGRAPHY

I grew up in Richmond, Virginia and received my Bachelor's degree in marine science with a concentration in chemistry from North Carolina State University in May 2015. During my undergraduate career, I began working as a research assistant in Dr. Chris Osburn's biogeochemistry lab. Working in the lab sparked my interest in marine biogeochemistry and inspired me to apply to graduate school and receive my Master's. I plan to stay in the environmental science field and study water quality.

ACKNOWLEDGMENTS

I would like to thank my graduate advisor, Dr. Christopher Osburn and the rest of my thesis committee, Dr. David DeMaster and Dr. Karen McNeal. I am thankful for the opportunity to learn, grow, and develop my skills in the field of marine biogeochemistry. I would also like to thank other collaborators and mentors, specifically Drs. Mike Montgomery and Tom Boyd for all of their help. Thanks to the Strategic Environmental Research and Development Program (SERDP) for funding this research. I would also like to thank Texas A&M Corpus Christi, University of North Carolina Institute of Marine Sciences, and Naval Research Laboratory – Key West for logistical support during sampling. Special thanks to all the past and present Osburn Lab group members for mentorship, advice, edits and support through this process. I would lastly like to thank my family for the constant love and support they have provided me, without them I would not be where I am today.

TABLE OF CONTENTS

LIST OF TABLES

LIST OF FIGURES

INTRODUCTION

Coastal waters provide a connection between freshwater systems and the open ocean (Abril et al., 2002; Bianchi and Bauer, 2011), and 87% of the land's surface area is connected to the coastal environment through estuaries and rivers (Bauer and Bianchi, 2011). An essential component of estuarine biogeochemistry is organic matter (OM). OM is made up of organic compounds derived from living and non-living plant, animal, and microbial material containing carbon, nitrogen, phosphorus, and sulfur (Stedmon et al., 2006). Organic carbon (OC) makes up ca. 50% of the OM pool, making it an important fraction to study because of its larger contribution compared to the other elements to the total OM pool. Additionally, OC contributes to the global carbon cycle through carbon burial, transformation processes to inorganic carbon (carbon dioxide), and export to the coastal ocean (Bianchi, 2006; Spencer et al., 2007; Bauer et al., 2013). OM transformations in estuaries and coastal waters have been researched extensively, although knowledge gaps remain in quantities of carbon transported from fresh waters to the coastal ocean (Goñi and Thomas, 2000; McKee et al., 2004; Benner and Amon, 2015). Traditionally, estuaries were thought of as a pipe that transported OM passively to the ocean, but in the last few decades numerous studies have demonstrated that estuaries are very dynamic systems that actively transform, produce, and alter OM (McKee et al., 2004; McCallister et al., 2006; Cole et al., 2007).

Chemical, physical, and biological processes modify OM as it is transported across the terrestrial – marine interface from land to ocean through estuaries. For example, salinity and temperature guide circulation patterns, which dictate residence time and distribution of water in an estuary and in turn the formation, transformation, and degradation of OM before

entering the coastal ocean (Bauer and Bianchi, 2011). Biological activity (e.g., plant, animal, algal, microbial) produces and re-mineralizes OM at rates that depend on many other factors including temperature, nutrients, and light availability (Peterson et al., 1994). Another major factor controlling the fate of OM in estuaries is photochemistry (Sulzberger and Kaiser, 2009). Photooxidation degrades OM changing its chemical character (Osburn et al., 2011). Areas with greater amounts of ultraviolet radiation typically have more photodegradation of OM (Tedetti and Sempere, 2006). Also, land cover that is continuously changing, temporally and spatially, influences these transformation processes via allochthonous or autochthonous inputs of OM to coastal systems (Bauer and Bianchi, 2011).

The interaction between biological and physicochemical variables with the chemical character of OM depends on the environmental setting. OM is commonly classified, based on particle size, into two main fractions, dissolved organic matter (DOM) and particulate organic matter (POM). The size classes behave differently in natural environments (Abril et al., 2002; Osburn et al., 2012). DOM is operationally defined as organic matter that passes through a 0.7-μm-porosity filter, while the POM is the organic material that is collected on the filter. Colloids, viruses, bacteria, and small truly dissolved organic compounds constitute a large portion of DOM (Repeta, 2014). Due to the small size and complex composition, DOM is difficult to understand at a molecular level even though specific components of DOM (amino acids, sugars, ketones, and aldehydes) are commonly characterized (Hedges et al., 2000; Repeta, 2014; Benner and Amon, 2015). POM can either be organic material or a combination of inorganic and organic material bound together (Hedges and Keil, 1999). In some coastal waters, DOM is typically more degraded, often originating as recalcitrant, soil-

derived material (e.g., humic and fulvic acids), while POM typically is fresher, consisting of more labile material of recent biological (planktonic) production (Osburn et al., 2012).

OM sources to coastal waters can be described as autochthonous or allochthonous. Autochthonous is material produced within the system, whereas allochthonous material corresponds to that being brought in from an external source (Asmala et al., 2013). Autochthonous OM in an estuary originates mainly from primary production by local phytoplankton and plants. Allochthonous sources include terrestrial material from the freshwater endmember and marine phytoplankton from the oceanic endmember (Bianchi, 2006). An area may have various endmembers influencing the mixing dynamics within the system that affect the quality or quantity as well. A region's surroundings including vegetation and the type of coastal waters (e.g., lagoonal estuary, river dominated estuary) control the quantity of allochthonous and autochthonous material in coastal waters, as well as the characteristics of its source, which in turn influence its chemical character. For example, in temperate/subtropical environments, brackish/salt marshes are a major source of organic carbon to coastal waters, including cordgrasses and seagrasses, like *Spartina alterniflora* (Goñi and Thomas, 2000). In contrast, mangroves, such as *Rhizophora mangle* and *Avicennia germinans* and seagrasses, like *Thalassia testudinum,* are examples of vegetation that provide source material to a tropical estuary (Tremblay et al., 2007).

It is well known that most terrestrial material does not persist in the open ocean**,** which highlights the importance of coastal waters as a hotspot for transformation and degradation of terrestrial OM (Hedges et al., 1997). Along with these transformations processes, its essential to understand the coastal carbon cycle, which includes the re-

mineralization of OC to inorganic carbon (e.g., the climatically active gas CO_2) as well as the net fluxes of carbon (Goñi and Thomas, 2000; Mannino and Harvey, 2000; McKee et al., 2004; Bauer and Bianchi, 2011). However, many questions remain about how different biological and physicochemical factors affect the fate and flux of organic matter through estuaries and adjacent coastal waters (Cole et al., 2007; Benner and Amon, 2015). For example, few studies have looked at estuaries and coastal waters in a comparative sense and have attempted to link climate to OM fluxes and processes within the freshwater to marine continuum.

To address the uncertainty of the role of large-scale variables such as climate compared to local environmental variables, the overarching hypothesis for this study was that varying climatic regions will impact OM dynamics (dissolved and particulate) as they are transported to the coastal ocean. The main objective of this research was to compare the quantity and quality of dissolved and particulate organic matter pools (DOM and POM, respectively) among five estuarine and coastal sites from varying climatic regimes. Here, "estuary" is defined in its broadest sense: a representation of the terrestrial to marine interface with some systems being entirely connected (e.g., coastal plain) and others being disconnected (e.g., coastal waters surrounding Key West, FL). It was hypothesized that the Köppen climate classifications would influence the DOM and POM quantity and quality in varying regions; therefore, these OM properties would be regionally dependent.

The main questions for this research used to address this hypothesis were as follows:

1. Do the regional climate classifications influence the quantity and quality of DOM and POM in the five sites?

2. What are the differences between quantity and quality in the two dissolved and particulate OM size fractions among the five sites?
3. How do different surroundings (e.g., vegetation, freshwater inflow) influence the chemical character of OM at the five contrasting sites?

The study sites chosen for this research varied regionally with respect to Köppens climate classification system, which is based on regional vegetation, and annual precipitation and air temperature (Kottek et al., 2006). The five regional sites were as follows with their climate classification: 1) the Lower Outer Banks estuarine system in North Carolina (NC, humid subtropical) with samplings from the Newport River, the Newport River Estuary, the White Oak River Estuary, the New River Estuary, Bogue Sound, a brackish marsh, and Onslow Bay in the coastal Atlantic Ocean; 2) three river estuarine systems (Cooper, Ashley and Wando River) in South Carolina (SC, humid subtropical), which flow through Charleston Harbor Estuary, into the coastal ocean of the South Atlantic Bight; 3) an urban canal, a mangrove dominated tidal mudflat environment, the channel next to this mudflat, and Aransas Pass in Texas (TX, humid subtropical); 4) coastal waters around the Florida Keys, including a mangrove pond on No Name Key, and the coastal ocean in Florida (FL, tropical savanna); and 5) Kahana Bay estuarine system in Hawaii (HI, tropical rainforest).

Several optical and chemical techniques were used to gain a better quantitative and qualitative understanding of the chemical character, or "quality," of the OM in these coastal waters. Absorbance and fluorescence measurements provide information on the chemical characteristics of DOM and POM and their sources from the different biological and physicochemical regimes. DOM that contains conjugated structures, often found in aromatic

compounds, characterizes a small fraction of the overall DOM, termed chromophoric DOM (CDOM). CDOM is the fraction of DOM that absorbs light, specifically at ultraviolet and blue-light wavelengths <400 nm (Weishaar et al., 2003). Similarly, some compounds in POM can also absorb light; however prior to analysis the POM must be base extracted into a solution (BEPOM) in order to be measured (Brym et al., 2014). The absorption spectra can provide insight as to the molecular weight and aromaticity of CDOM and BEPOM (Stedmon and Nelson, 2015). Fluorescence spectroscopy measures the fluorescent OM in DOM and POM. Excitation emission matrices (EEMs) from the fluorescent OM have been extensively used to characterize freshness and broad chemical character, such as protein-like or humic-like (Coble, 1996; Yamashita et al., 2008). Dissolved and particulate organic carbon (DOC, POC) concentrations can be measured to determine the amounts of OC in estuaries and coastal waters. Lastly, stable carbon isotope ($\delta^{13}C$) analyses coupled with elemental carbon to nitrogen (C:N) ratios were used to identify sources of OM at the bulk level as opposed to only the subset detected by absorbance and fluorescence (Bianchi, 2006; Osburn and Stedmon, 2011). Each method contributed to the overall goal of examining the quantitative and qualitative properties of DOM and POM at each of the five locations as a function of climate classifications.

STUDY SITES

Sampling was conducted seasonally among five climatic regions (Table 1). The North Carolina sampling took place in April 2014, August 2014, November 2014, and August 2015. The South Carolina sampling was conducted in June 2011, whereas the Texas sampling took place in September 2015. The Florida sampling was conducted in May 2013, August 2013, November 2013, and October 2015. Lastly, the Hawaii sampling occurred in July 2010 and August 2011. Mean air temperatures and total precipitation for the seven days prior to and during sampling are listed in Table 1. Site abbreviations, climate classifications, latitudinal locations along with annual mean air temperatures and annual mean precipitation for years sampled are listed in Table 2 to provide context for the weather conditions during each year sampled.

North Carolina (NC) sampling was done in various coastal waters in local systems located along the Lower Outer Banks including: the Newport River, Newport River Estuary, Bogue Sound, White Oak River Estuary, New River Estuary, a brackish marsh wetland that fringed the Newport River Estuary, and the coastal Atlantic Ocean (Table 3). The Newport River Estuary, White Oak River Estuary and New River Estuary are all considered coastal plain estuarine systems. Coastal plain estuaries are described as low relief areas that are greatly influenced by outflow of sediments thus creating a river valley (Bianchi, 2006). The Newport River and Newport River Estuary have the same watershed area of approximately 198 km^2, though smaller watersheds along the northern and southern coastal boundaries also impact the estuary (Revsbæk et al., 2014). The Newport River Estuary is relatively shallow with a mean depth of 1 m, surrounded by brackish marsh wetlands (Kirby-Smith and

Costlow, 1989). The White Oak River Estuary is slightly deeper, with an approximate depth between 1 to 2 m and surrounded by brackish marsh forested vegetation (Land and Paull, 2001) and a watershed area of 959 km^2 (Revsbæk et al., 2014). The New River Estuary has a watershed area of 1251 km^2 (Revsbæk et al., 2014), a mean depth of 0.9 m, and a mean monthly river flow of 277,000 m^3 d^{-1} (Engle et al., 2007). All three of these estuaries (Newport River Estuary, White Oak River Estuary, New River Estuary) border Bogue Sound. Bogue Sound has a watershed area of 1830 km^2 and a mean water depth of 1.8 m (Engle et al., 2007). The barrier islands, constraining Bogue Sound to the south, prevent a large exchange with the coastal ocean except for semi-diurnal tidal influences (Bianchi, 2007). The NC coast is characterized as micro-tidal, ranging approximately from 1 to 2 m (Moslow and Heron Jr., 1994).

Samples in South Carolina (SC) were collected from three river estuarine systems (the Cooper, Ashley and Wando River Estuaries) that all drain into the Charleston Harbor. Additionally, samples were collected on the continental shelf of the South Atlantic Bight as a coastal marine endmember. Similar to three of the estuaries in NC, SC is also considered a coastal plain estuary because of the low relief river valleys. Of the three river estuarine systems, the Cooper River Estuary has the largest watershed area (1870 km^2), followed by the Ashley River Estuary (1020 km^2), and lastly the Wando River Estuary (292 km^2; Revsbæk et al., 2014). Charleston Harbor has a mean depth of 3.8 m and mean monthly river flow of 1.37×10^7 m^3 d^{-1} from the three river estuaries (Engle et al., 2007). Similar to NC, SC has semi-diurnal tidal influences over a micro-tidal range.

Samples near Corpus Christi, Texas (TX) were collected from four sites: an urban canal, a tidal mudflat, a channel adjacent to the mudflat, and Aransas Pass. The urban canal, which drains into Oso Bay, has inputs from local wastewater discharge and has a watershed area of approximately 549 km^2 (Revsbæk et al., 2014). The tidal mudflat is located in the Aransas Pass Nature Preserve and disconnected from any surrounding channels, consequently isolated from Aransas Pass except during flushing events. The mudflat is very shallow and dominated by black mangroves (*Avicennia germinans*), while Aransas Pass is the closest connection to the coastal Gulf of Mexico. The mudflat is bordered by Aransas Bay to the north, but receives the largest influence from Corpus Christi Bay to the south. Residence times of Aransas Bay and Corpus Christi Bay are approximately 360 and 356 days, respectively (Solis and Powell, 1999). Diurnal tides along the coastal areas of Corpus Christi ranged from 0.5 to 0.7 m, so they are classified as micro-tidal (Solis and Powell, 1999).

Florida sampling (FL) was conducted in coastal sites around the Florida Keys, No Name Key mangrove pond, and coastal Gulf of Mexico. Examples of coastal sites included areas near Trumbo Point, Fleming Key, Dredgers Key and Boca Chica Field. The mangrove area on No Name Key was an isolated pond surrounded by red mangrove vegetation (*Rhizophora mangle*) that was not connected to any coastal waters. This mangrove environment was deeper and more secluded than the TX tidal mudflat. There were no surface freshwater inputs among the local areas sampled (precipitation was not sampled in this study). Similar to TX, FL has diurnal micro-tidal influences ranging from 0.5 to 0.7 m (Solis and Powell, 1999).

A Hawaiian (HI) estuary was sampled along a salinity gradient of the Kahana stream flowing into the Kahana Bay, which is located on the northeast side of Oahu. Kahana Bay has inputs from a local stream, where the sampling was conducted. Additionally, the area sampled has terrestrial submarine groundwater inputs (Garrison et al., 2003). The salinity gradient along the 100m long sampling transect was steep, reflective of the tropical rainforest climate. The Kahana Bay and stream are surrounded by local forested woody vegetation, and tides are semi-diurnal in this area.

MATERIALS AND METHODS

Sampling

Whole water samples were collected at the five coastal regions during 2011 through 2015: NC, SC, TX, FL and HI. Members of the Osburn lab group or collaborators on the project supported by the Strategic Environmental Research and Development Program (SERDP) collected samples in 1 L pre-rinsed polycarbonate bottles from estuarine and coastal waters. SC included samples collected at surface, middle and bottom water depths, while at the other sites only collected surface water samples. Prior to collection, bottles were cleaned in a detergent bath, rinsed with ultrapure lab water (Milli-Q water), and dried. During sample collection, bottles were pre-rinsed three times with water from each sampling site. Samples were stored on ice for multiple hours until laboratory methods could be performed.

Laboratory Methods

After collection, a known volume of whole water sample was filtered through a pre-combusted 0.7 μm Whatman glass fiber filter (GF/F). The filter was stored frozen in a 15 mL polypropylene centrifuge tube until processing for base-extracted particulate organic matter (BEPOM; see below). Filters were stored frozen for a minimum of 3 weeks up to a maximum storage time of 3 years. The GF/F filtrate was stored frozen in a 60 mL polycarbonate bottle ranging from 1 week to 3 months until measurements on optical properties (fluorescence and absorbance) could be performed for CDOM. A second aliquot of filtrate was acidified with 85% phosphoric acid (H_3PO_4) to a pH of 2 and stored at 4°C until measurement for dissolved

organic carbon (DOC) concentration and stable carbon isotopes of DOM (δ^{13}C-DOM), while a second GF/F filter was collected and stored frozen for later analysis of particulate organic carbon (POC), particulate nitrogen (PN) and stable carbon isotopes for POM (δ^{13}C-POM). The GF/F filters were stored frozen for a minimum amount of time of 10 months to a maximum of 5 years.

Base Extracted Particulate Organic Matter (BEPOM)

In the laboratory, the material collected on the GF/F filter was base extracted in 10 mL of 0.1 *N* sodium hydroxide (NaOH) for 24 hours at 4°C. After the 24-hour period, the solution was neutralized with concentrated hydrochloric acid (HCl) and filtered through a 0.2 μm filter (polyethersulfone, PES, Osburn et al., 2012; Brym et al., 2014). Absorbance and fluorescence of the extracted filtrate were measured the same day as the solution was neutralized.

Absorbance and Fluorescence spectroscopy

CDOM and BEPOM absorbance were measured from 200-800 nm using a Varian Cary 300 UV spectrophotometer with a 1 and 10 cm cell, respectively. Longer cell lengths were used for samples with a lower signal of organic matter. CDOM samples run on a 1 cm cell that exceeded absorption of 0.4 at 240 nm were diluted and re-run. If the absorbance at 400 nm was ≤0.002 in the 1 cm cell, the samples were re-run on a 10 cm cell. Milli-Q lab water was used to blank correct the CDOM samples. BEPOM samples were blank corrected with a solution of neutralized NaOH that was stored for 24 hours, similarly to the extracted

samples. Napierian absorption for CDOM and BEPOM was quantified at 254 nm (a_{254}d and a_{254}p, respectively) in units of inverse meters (m^{-1}) using equation 1. The absorbance of the blank $A(\lambda_{blank})$ was subtracted from the absorbance of the CDOM or BEPOM sample, $A(\lambda_{sample})$, and divided by the pathlength (L) of the cell. Lastly, the Napierian absorption value, $a(\lambda_{sample})$ was calculated by multiplying by 2.303 to convert Napierian values to their respective decadal absorption coefficient. The precision of the absorption measurements was to two decimal places based on consistency with replicate measurements.

$$a(\lambda_{sample}) = \frac{A(\lambda_{sample}) - A(\lambda_{blank})}{L} x\ 2.303 \quad (1)$$

The slope ratio (S_R) for CDOM and BEPOM (S_Rd and S_Rp, respectively) and absorption at 254 nm (a_{254}) were computed using MATLAB 2016a (Mathworks, Natick, MA). The S_R is the ratio of absorbance between 275-295 nm to absorbance between 350-400 nm and is a qualitative indicator for molecular weight of the sample. Larger S_R values indicate samples have a low molecular weight, and samples with smaller S_R values have a high molecular weight (Helms et al., 2008). A proxy used for dissolved organic carbon (DOC) concentrations was a_{254}d values. A sample's decadal a_{254}d (m^{-1}) value divided by its DOC concentration (mg L^{-1}) was used to calculate its specific UV absorbance at 254 nm ($SUVA_{254}$, L mg C^{-1} m^{-1}), which is an index of its aromaticity (Weishaar et al., 2003; Wagner et al., 2015).

CDOM and BEPOM fluorescence samples were measured in a 1 cm quartz cell (Starna, Inc., Atascadero, CA) using a Varian Eclipse fluorescence spectrophotometer. Excitation was scanned from 240-450 nm with 5 nm intervals and emission was scanned from 300-600 nm with 2 nm intervals. The spectra were compiled in excitation emission

matrices (EEMs) that were examined using parallel factor analysis (PARAFAC). Samples were measured at different voltages depending on each sample's signal intensity. The lamp voltages included 700, 750, 800, 850, and 900 V with scan speeds of 1200 and 2400 nm min^{-1} depending on the voltage. The slit widths were 5 nm for excitation and emission modes. Fluorescence intensity was normalized to quinine sulfate units (ppb QSU) after correcting for the instrument's water Raman signal (Lawaetz and Stedmon, 2009). Similar to absorbance measurements, Milli-Q lab water was used to blank correct the fluorescence CDOM samples; whereas a solution of neutralized NaOH was used to blank correct the BEPOM samples.

DOC and Stable Carbon Isotopes (δ^{13}C-DOM)

DOC concentrations, [DOC], were measured on an OI Analytical 1030D Aurora total organic carbon analyzer, coupled to a Thermo Delta V Plus Isotope Ratio Mass Spectrometer (IRMS) for measuring δ^{13}C-DOM values. Prior to analysis, the samples were sparged with Argon gas to eliminate dissolved inorganic carbon. [DOC] were blank corrected and calculated via a linear regression with known caffeine concentrations ranging from 1 to 60 mg C L^{-1}, which is well within the limit of detection for a linear response. δ^{13}C-DOM values (in units of ‰) were blank corrected and normalized to the Vienna Pee Dee Belemnite (VPDB) scale using a linear fit of IAEA 600 caffeine (-27.7±0.04‰) and IAEA C6 sucrose (-10.8±0.03‰) International Atomic Energy Agency (IAEA) standards. A standard curve was run approximately every 35 samples, and the reproducibility of the curve fit was assessed through correlation coefficients (r^2) ≥ 0.995. No samples analyzed were less than 1 mg C L^{-1}, thus a low carbon standard such as a Hansell deep-sea reference (DSR) was not

required. The precision for [DOC] and δ^{13}C-DOM values were ±0.4‰ based on reproducibility and calibration to the sucrose standard and Hansell Deep Sea Reference material. Milli-Q blanks were run every 7 samples for quality control and assurance of the instrument.

POC, PN concentrations and δ^{13}C-POM

GF/F filters, analyzed for particulate organic carbon (POC) and particulate nitrogen (PN), were dried at 30°C for 24 hours. POC concentrations [POC] and PN concentrations were measured on a Thermo Finnigan Flash Series 1112 Elemental Analyzer (EA). This instrument was coupled with an IRMS to measure δ^{13}C-POM values of the sample's [POC] and PN concentrations. Acetanilide, L-glutamic acid, caffeine, oxalic acid, and sucrose standards were used to standardize the sample analyses. Standards that weighed between 0.04 to 0.60 mg were prepared in 4x6 mm (width x height) tin capsules. The dried filters were folded and analyzed in 10x12 mm tin capsules (width x height). Acetanilide standards (carbon content of 71.09% and nitrogen content of 10.36%) were used to determine the EA carbon and nitrogen peak locations and to calibrate the carbon and nitrogen-working curve for each sample. L-glutamic acid is a United States Geological Survey (USGS-40) standard, caffeine (600) and sucrose (C6) are IAEA standards, and oxalic acid is a National Institute of Standards and Technology (NIST-4990C) standard. L-glutamic acid, caffeine, oxalic acid and sucrose have $\delta^{13}C_{VPDB}$ values of -26.39‰, -27.77‰, -17.8‰, and -10.8‰, respectively, and were linearly fit with raw δ^{13}C-POM values, creating a standard curve to obtain δ^{13}C-POM values for samples corrected to the VPDB scale. (Hereafter, all δ^{13}C values are

corrected to VPDB.) Similar to [DOC] and δ^{13}C-DOM values, the precision for [POC] and δ^{13}C-POM values were ±0.4‰ based on reproducibility and calibration to known standards. Molar ratios for carbon and nitrogen were computed and used to determine the bulk elemental C:N ratio for each sample.

Statistical Modeling

An analysis of variance (ANOVA on Ranks) was performed on the nonparametric data to assess differences among sites for the quantitative and qualitative geochemical measurements listed above. These measurements at the various sampling locations included CDOM a_{254}d values, BEPOM a_{254}p values, [DOC], [POC], CDOM S_Rd values, BEPOM S_Rp values, δ^{13}C-DOM values, δ^{13}C-POM values, CDOM $SUVA_{254}$ values, and POM molar C:N ratios. The Dunn's Test was used to determine which sites were significantly different from each other.

The DOMFluor toolbox in MATLAB 2016a was used to conduct parallel factor analysis (PARAFAC) on the multivariate dataset of EEMs. PARAFAC modeling decomposed a dataset of organic matter CDOM and BEPOM EEMs into components of varying fluorescent patterns. These patterns have been observed to differ depending on the sources to, and transformations of allochthonous or autochthonous OM within aquatic environments. Three PARAFAC models were created, one with both CDOM and BEPOM samples, one with CDOM samples only, and one with BEPOM samples only. Degradation experiments were performed at three sites (NC, TX, and FL), and the associated EEMs were used in the PARAFAC modeling. Fluorescence values were normalized to total fluorescence

for each model. All three models were run for 3-8 components, however the correct number of components was determined by checking the loadings and residuals of the samples. The loadings were plotted to see if there were outliers that were largely different from other samples within the dataset. Outliers were determined as samples with a leverage of 0.2 or greater and were removed from the model. Once outliers were removed, the model was re-run. The right number of components was determined once minimal scattering was observed in the residuals. If peaks were present in the residuals, then the model was incorrectly fit for the right number of components. Finding the right number of components is important because if too few or too many components were validated, then there could be overlapping components or modeled artifacts, respectively (Stedmon and Bro, 2008). The split half analyses were done by splitting the data in half and modeling both halves to test for the robustness of the model. Tucker's Congruence Coefficient measured the similarity among emission and excitation loadings to determine the number of validated components (Lorenzo-Seva and Berge, 2006). A random initialization using 10 models was performed to ensure that the fit was the sum of the least squares result (Stedmon and Bro, 2008; Osburn et al., 2015).

Once the model was validated, the components were compared on OpenFluor (http://www.openfluor.org), a database that includes PARAFAC models from published papers (Murphy et al., 2014). Each component was individually compared to components from published models through the excitation and emission loadings at a 95% confidence interval using Tucker's Congruence Coefficient. Comparing components to published research helps identify the source of the components and their ubiquity across different

aquatic ecosystems. Models in OpenFluor include components from coastal systems, salinity gradients, and open ocean sites. Three models were created and compared in OpenFluor. The first includes all CDOM and BEPOM samples (Model 1), the second includes only CDOM samples (Model 2), and the third model consists of only BEPOM samples (Model 3).

Principal Component Analysis (PCA) is another statistical test to understand variation within multivariate datasets (Bro and Smilde, 2014). PCA, through the PLS Toolbox in MATLAB 2016a, decomposed the PARAFAC results along with other variables such as salinity and measurements including a_{254}, S_R, $SUVA_{254}$, OC concentrations, C:N ratios, and $\delta^{13}C$ values. Prior to modeling, the data was auto-scaled, which subtracted out the mean then divided by the unit standard deviation, to ensure that all variables were analyzed on a similar scale. Before modeling, PCA also performed a cross-validation to test the robustness of the dataset. The cross-validation took half of the data then mathematically predicted the missing half of data. Depending on the prediction, there can be a high or low cross-validation error, or Root Mean Squared Error of Cross-Validation (RMSECV). After auto-scaling and cross validating, the data were modeled. The lowest RMSECV determined the number of principal components that were used during modeling. The PCA model output included principal components that explain a certain percentage of the variation in the overall dataset. Once the amount of principal components was set, the data were then re-modeled and analyzed through the scores, loadings, and the residuals of the samples. The scores correspond to each data point modeled, the loadings indicate the weighted averages from that data, and the residuals provide information concerning unexplained variation. Outliers were removed if they had high values, outside of the 95^{th} confidence limit, when scores were plotted against

residuals. If outliers were removed, the model was re-run. The main results of the PCA analysis were interpreted from the scores and loadings associated with principal component's 1 and 2 (PC1 and PC2).

RESULTS

CDOM and BEPOM absorption concentrations

Mean $a_{254}d$ values from the various regions were ranked in descending order as follows: NC>TX>FL>SC>HI (Fig. 1A). However, within site variation occurred due to differences in these coastal ecosystems, proximity to land, and sampling frequency at the five sites. For example, sampling in NC was done four different times in river estuarine systems, a brackish marsh, and the coastal ocean, whereas HI was only sampled twice in one estuarine system, Kahana Bay (Table 3). In the humid subtropical climates of NC, SC, and TX, and the tropical savanna climate of FL the highest CDOM absorbance occurred in areas closest to land such as rivers and wetland environments. For example, the Newport River and water adjacent to the brackish marsh that fringed the Newport River Estuary in NC (349.28±78.97 m^{-1} and 268.19 m^{-1}, respectively); the Ashley River Estuary in SC (25.86±0.10 m^{-1}); the urban canal and the tidal mudflat in TX (58.17 and 72.48 m^{-1}, respectively); and, the mangrove pond on No Name Key in FL (125.65±16.72 m^{-1}; Table 3). Additionally, the NC coastal waters had significantly higher $a_{254}d$ values than three of the four other sampling sites (SC, FL and HI; $p < 0.05$; Table 4), with values that ranged from 28.96±9.56 m^{-1} in the White Oak River Estuary to 112.72±97.21 m^{-1} in the Newport River Estuary. These locations also experienced significant within-site variability as demonstrated by the high standard deviations associated with these means (Table 3). In NC, SC, TX, and FL the lowest $a_{254}d$ values were found in the coastal marine samples (Table 3). Lastly, the Kahana Bay estuary in HI had the lowest mean $a_{254}d$ values compared to the other four sites (4.83±1.95 m^{-1}), and were similar to the lowest $a_{254}d$ values observed in NC, SC and FL coastal marine areas

(2.66, 3.62±0.65, and 5.09±0.65 m^{-1}, respectively; Table 3).

NC had the highest mean $a_{254}p$ values, followed by TX>HI>SC>FL (Fig. 1B). The highest $a_{254}p$ values in NC, TX and FL were from the same local areas that had the highest $a_{254}d$ values (Table 3). However, the mean $a_{254}p$ values between NC and TX were found to be significantly higher than values measured in FL, determined by an ANOVA on Ranks ($p < 0.05$; Table 4). Kahana Bay (HI) had a mean $a_{254}p$ value of 0.49±0.30 m^{-1}, comparable to the mean $a_{254}p$ values in two of the SC estuaries (Cooper River Estuary and Ashley River Estuary), but lower than any of the mean values from the NC estuaries (Table 3). The $a_{254}p$ values in NC were found to be significantly higher than values in SC (ANOVA on Ranks, $p < 0.05$; Table 4). The estuaries in SC ranged between mean values of 0.29±0.03 m^{-1} in the Charleston Harbor to 0.94±0.98 m^{-1} in the Wando River Estuary (Table 3). Similar to $a_{254}d$ values, the lowest $a_{254}p$ values found among four of the regions (NC, SC, TX, and FL) were from the coastal marine waters (Table 3).

Organic carbon (OC) concentrations

The highest [DOC] was found in TX, followed by NC, FL, SC, and HI, generally in freshwater or wetland environments (Fig. 1C). For example, in TX the highest [DOC] was a tidal mudflat (42.7 mg L^{-1}), and in NC, the highest [DOC] values occurred in the Newport River and waters adjacent to a brackish marsh (31.8±8.40 and 27.2 mg L^{-1}, respectively; Table 3). The overall [DOC] between NC and TX did not differ significantly using an ANOVA on Ranks, however, NC and TX [DOC] were significantly higher than were HI and FL [DOC] ($p < 0.05$; Table 4). In FL the wetland mangrove pond on No Name Key had the

highest [DOC] (15.0±1.65 mg L^{-1}), similar to results in NC and TX. The estuaries in SC had comparable [DOC] ranging from 2.4±0.56 mg L^{-1} in the Wando River Estuary to 3.5±0.92 mg L^{-1} in the Cooper River Estuary (Table 3). The lowest [DOC] in three of the five regions (NC, SC, and FL) were found in the coastal marine waters (Table 3). Similar to a_{254}d results, the lowest mean [DOC] from the five regions was found in Kahana Bay, HI (1.4±0.41 mg L^{-1}; Table 3).

Regional [POC] was lower than [DOC], following the trend TX>NC>FL>SC (no data for HI; Fig. 1D). [POC] in the four sites was less variable than [DOC] with a range from the highest value, 5.3 mg L^{-1}, found in the urban canal in TX to the lowest value, 0.2 mg L^{-1}, found in a coastal marine sample in NC (Table 3). Similar to [DOC], the highest [POC] was found in coastal waters influenced by fluvial inputs or near wetland environments. TX and NC [POC] data were not significantly different based on an ANOVA on Ranks ($p < 0.05$; Table 4), with the highest [POC] values found in the urban canal in TX (5.5 mg L^{-1}) and the New River Estuary in NC (4.4±2.25 mg L^{-1}). The other coastal waters in NC, with the exception of the coastal marine sample, had [POC] ranging from 1.0±0.71 to 2.4 mg L^{-1} (Table 3). The highest [POC] in FL was found in the mangrove pond, and the lowest [POC] was found in the channels around the Florida Keys (0.5±0.59 mg L^{-1}; Table 3). The Ashley River Estuary had the highest [POC] in SC (1.3±0.03 mg L^{-1}), and the other estuaries had [POC] that ranged from 0.8±0.06 to 1.0±0.30 mg L^{-1} (Table 3). In the three regions with humid subtropical climates (NC, SC, and TX), the only significant difference was observed between NC and SC [POC] ($p < 0.05$; Table 4). Additionally, in NC and SC the lowest [POC] was found in the coastal marine waters (Table 3).

Linear regression analysis was conducted on the five region's $a_{254}d$ values and [DOC] to determine significantly linear trends (Table 5). Additionally, an ANCOVA with Tukey's post-test was performed to identify significant differences among the five region's slopes of $a_{254}d$ values and [DOC]. In TX, the urban canal sample was excluded when fitting a linear regression because it was dissimilar to the other sampling environments, which were collected in or around Corpus Christi Bay. All five region's $a_{254}d$ values vs. [DOC] were found to have statistically significant slopes with correlation coefficients (r^2) ≥ 0.639 (Table 5). However, the ANCOVA results found that TX samples had a significantly lower slope than the four other sites ($p < 0.05$; Table 6).

Along with regional comparisons, linear regression analysis was conducted on $a_{254}d$ values and [DOC] for seasonal samplings for each of the five study sites to look for differences in the $a_{254}d$ vs. [DOC] relationship over seasons (Table 7). In FL, a linear regression was not fit to the November 2013 sampling because there were only two samples. Exceptions to the strong linear trends were found in three of the five regions (NC, SC, and FL). For example, April 2014 in NC and May 2013 in FL did not have statistically significant trends, whereas SC samples had a weaker correlation in $a_{254}d$ vs. [DOC], although still significant (Table 7). When comparing the significant seasonal slopes, NC August and November 2014, FL, and HI samples appeared to have the most similar linear relationship (Figs. 2A and 2B). In contrast, TX samples and NC August 2015 samples plotted differently, appearing to show two additional linear trends (Fig. 2A). Lastly, SC seemed to show minimal change in CDOM concentration per unit [DOC], displaying yet another linear trend than the other three trends (Fig. 2B).

ANCOVA followed by Tukey's post-test was then used to determine any significant differences in the slope of the $a_{254}d$ vs. [DOC] relationship among different seasonal samplings for each region sampled. There were no significant differences in slopes observed over the various seasonal samplings in FL or HI ($p < 0.05$; Table 8). In NC, the slope for the $a_{254}d$ vs. [DOC] relationship from the August 2015 sampling was significantly different among the four samplings, which included a repeat sampling from August 2014 ($p < 0.05$; Table 8). There were no other significant differences observed in slopes within each region's seasonal samplings.

Trends in [DOC] and [POC] with salinity

In order to evaluate the mixing dynamics of the coastal waters studied, linear regressions of [DOC] and [POC] vs. salinity were performed. Conservative mixing was defined as [DOC] or [POC] vs. salinity data points that fell within a 95% confidence interval for each regression (dashed lines, Figs. 3 and 4). [DOC] or [POC] outside of the 95% confidence intervals were denoted as outliers, and therefore considered to show non-conservative behavior that may result from in situ processes or additional sources.

For NC estuaries and coastal waters, trends in [DOC] showed clear decreases with salinity over all seasons sampled and trends were largely conservative (Fig. 3). Bogue Sound lacked direct riverine inputs and therefore did not exhibit two-endmember mixing (Fig. 3I), in contrast to the New River Estuary and Newport River Estuary. Additional areas in NC such as the White Oak River Estuary, the coastal waters of Onslow Bay, and a brackish marsh that fringed the Newport River Estuary also exhibited conservative mixing

relationships (Figs. 3A, 3C, 3E, and 3G). Among the samplings in NC, there were no consistent linear trends over the varying seasons. August 2015 sampling had more outliers than August 2014, including the Newport River Estuary samples above the mixing line with [DOC] of 22.7 and 19.1 mg L^{-1} at salinities of 23.8 and 31.1, respectively (circles in Fig. 3G). All of the samples in Bogue Sound had relatively low [DOC] (Fig. 3I).

Similar to NC [DOC], the Charleston Harbor and the three river inflows had decreased [DOC] with increased salinity (Fig. 4A). Linearity in SC was weaker than for NC [DOC] vs. salinity relationships with an r^2 value of 0.763 vs. 0.931. Conversely, in TX coastal waters, [DOC] increased over the salinity gradient, with the highest [DOC] observed at the highest salinity, which is common for Texas estuaries situated in semi-arid environments (Fig. 4C; Bianchi et al., 1999). Mixing lines were not used because the areas sampled were not over a continuous estuarine gradient, and therefore would not be representative of the mixing dynamics. The [DOC] at the lowest salinity (18.7 mg L^{-1} at 2.8) was collected in an urban canal that drains into the Oso Bay (circle in Fig. 4C). The sample with the highest [DOC] (42.7 mg L^{-1} at 41.9) was collected from a disconnected tidal mudflat, isolated from the adjacent channel, within the Aransas Pass Nature Preserve (diamond in Fig. 4C). [DOC] from the channel adjacent to the tidal mudflat and Aransas Pass plotted similarly, ranging in salinity from ~31 to 33. Similar to NC and SC, Kahana Bay in HI showed a similar decrease [DOC] over the salinity gradient, however, there was a weaker correlation (r^2=0.720; Fig. 4G) than NC samplings (Fig. 3A, 3C, 3E, and 3G), and SC (Fig. 4A). Similar to FL, both HI sampling dates (June 2010 and August 2011) were plotted together due to the similarity in the range of [DOC] with salinity. For example, in June 2010

and August 2011, mean (±SD) [DOC] were 1.3±0.29 and 1.4±0.51 mg L^{-1}, respectively.

DOC at coastal sites sampled around the tropical savanna climate of the Florida Keys (FL) were similar to those in the humid subtropical climate of TX locations around Corpus Christi Bay and Aransas Pass, with high [DOC] – 16.3, 15.6, and 13.2 mg L^{-1} – occurring at high salinities of 42.6, 30.1, and 36.3, respectively (Fig. 4E). These samples were taken from a mangrove pond that was disconnected from open water, hence the small range in salinity, including one observation of hypersalinity. Generally, the salinity range in FL samples (30.1 to 42.6) was due to a lack of freshwater input to the coastal waters around the keys near Key West; therefore, a clear mixing line could not be determined (Fig. 4E). Also note that the various [DOC] from different sampling years in FL were not plotted separately like NC because of the similarity in [DOC]. Clustering of these values indicated a more homogenous distribution of DOC in coastal waters around Key West stretching out to the open Gulf of Mexico. [DOC] >10 mg L^{-1} from the mangrove pond were similar to mangrove tidal mudflats, although mangrove vegetation in FL was dominated by red mangroves (*Rhizophora mangle*), different from the black mangroves (*Avicennia germinans*) that populate the TX region. In FL, the disconnected ponds have greater influences on increased [DOC] from local mangrove vegetation and hypersaline due to their isolation from frequent exchange with coastal waters, which facilitated evapo-concentration. The [DOC] <10 mg L^{-1} were collected around the Florida Keys close to land, as well as from coastal marine waters.

Concentrations of POC in NC estuaries and coastal waters, decreased with increasing salinity, similar to [DOC] results (Fig. 3). However, [POC] demonstrated greater variability and typically non-conservative behavior with salinity as well as decreased magnitudes in

[POC] during all four sampling times (Figs. 3B, 3D, 3F, and 3H) and within Bogue Sound (Fig. 3J). Similar to [DOC], the mixing lines were indicative of binary mixing in the New River estuarine system during April 2014, and the Newport River estuarine system during August 2014, November 2014, and August 2015 with contributions from the other coastal waters sampled (Figs. 3B, 3D, 3F, 3H, and 3J). Again, Bogue Sound was plotted separately due to varying [POC] behavior with salinity (Fig. 3J). August 2014 was the only seasonal sampling that had a significant linear trend (r^2=0.884; $p < 0.05$; Fig. 3D). In contrast to the other seasonal samplings, August 2015 [POC] showed a notable trend with the highest [POC] at mid-salinities, although not significant or linear (Fig. 3H). Bogue Sound [POC] was also variable compared to other sampling times, but generally had higher [POC] at mid-salinities (Fig. 3J).

In SC, [POC] decreased over the salinity gradient ranging from 1.0 mg L^{-1} at low salinity to 0.8 mg L^{-1} at the highest salinity (Fig. 4B). [POC] in the inflowing rivers to the Charleston Harbor and the Harbor itself behaved non-conservatively, showing greater variability than [DOC], resulting in a low r^2 value of 0.361, even though it was significant ($p < 0.05$; Fig. 4B).

Similar to the DOC results, TX and FL [POC] exhibited wide variability and surprisingly large values at high salinities of 30-40. The highest [POC] was found in the urban stream sample (5.3 mg L^{-1}) at a salinity of 2.8, whereas the lowest [POC] was found in Aransas Pass and in the channel adjacent to the mudflat (0.9±0.27 and 0.8 mg L^{-1}, respectively). The [POC] in the TX tidal mudflat sample was in between the urban stream and coastal waters (3.2 mg L^{-1}) at a salinity of 41.9.

Trends in DOM and POM quality

CDOM $SUVA_{254}$ values were highest in NC followed by SC>HI>FL>TX (Fig. 5E). Among the three humid subtropical climates, NC and SC coastal waters had significantly higher $SUVA_{254}$ values than coastal waters in TX (ANOVA on Ranks, $p < 0.05$; Table 10), including values ranging in the river estuarine systems from 2.11±1.29 to 4.92±1.03 L mg C^{-1} m^{-1} and 2.25±0.33 to 3.45±0.01 L mg C^{-1} m^{-1}, respectively. However, all three humid subtropical climates had the lowest values in the coastal marine waters (Table 9). In TX, the urban canal had the highest $SUVA_{254}$ value (1.35 L mg C^{-1} m^{-1}), although still 2 times lower than the highest values in NC or SC. The FL mangrove pond on No Name Key (3.63±0.14 L mg C^{-1} m^{-1}) fell in the range of values from the NC and SC river estuarine systems, but the overall FL coastal waters had significantly lower $SUVA_{254}$ values than SC values ($p < 0.05$; Table 10). Lastly, Kahana Bay in HI had a mean $SUVA_{254}$ value of 1.55±0.24 L mg C^{-1} m^{-1} (Table 9), which was not significantly different from any other region ($p < 0.05$; Table 10).

The slope ratio (S_R) has been shown to correlate inversely with molecular weight (Helms et al., 2008). CDOM in TX had the highest mean S_Rd values followed by SC>FL>NC>HI (Fig. 5A). In NC, SC, TX, and FL, the lowest values (≤ 1.0) were found in samples from wetlands or coastal waters with fluvial influences. Examples include the urban canal sample in TX (S_Rd value = 1.01), the Ashley River Estuary in SC (1.07±0), the mangrove pond on No Name Key, FL (1.12±0.06), and the Newport River in NC (0.74±0.04) (Table 9). No significant differences in CDOM S_Rd values were found among the regions, but the estuaries in NC had low S_Rd values (Table 10). These NC values ranged from 0.80 in the coastal water sample adjacent to the brackish marsh to 1.08±0.16 in Bogue Sound (Table

9). Similar to NC, the tropical rainforest climate of Kahana Bay samples had a mean S_Rd value of <1 (0.95±0.36; Table 9). The four SC estuaries flowing into the Charleston Harbor had CDOM samples with S_Rd values that had a range from 1.07±0 to 1.17±0.12 (Table 9). In almost every region (NC, SC, TX, and FL), the coastal marine samples had the highest S_Rd values, including Aransas Pass closest to the Gulf of Mexico in TX (1.61±0.56), the South Atlantic Bight in SC (1.39±0), the coastal marine areas in FL (1.22±0.05), and the coastal marine waters near the Atlantic Ocean in NC (1.82; Table 9).

In BEPOM, the highest S_Rp values were found in FL followed by TX>NC>HI (no data for SC; Fig. 5B). Similar to CDOM S_Rd values, BEPOM S_Rp values were not significantly different among the four sites ($p < 0.05$; Table 12). The highest S_Rp values in TX and FL were found in the urban canal and channels around the Florida Keys, respectively (Table 11). In contrast, the coastal marine waters in NC had the highest S_Rp value (4.63), whereas the other NC river estuarine systems ranged from 0.87±0.02 to 3.04±0.82. The lowest values in NC and TX were found in freshwater and wetland environments, specifically the Newport River in NC and the tidal mudflat in TX (Table 11), whereas, the lowest S_Rp value in FL was found in the coastal marine sample (2.55), the mean S_Rp value in Kahana Bay (1.93±0.90) fell within the range of values for NC estuaries and coastal waters.

Stable carbon isotopes ($\delta^{13}C$) can provide information concerning the sources of OM reaching aquatic environments, and were only available for three sites (NC, TX, and FL; Fig. 5C, Table 9). The humid subtropical climate of NC had a range of $\delta^{13}C$-DOM mean values, between -22.6 to -27.1±1.70‰ (Fig. 5C), with the most depleted values found in the Newport River and most enriched value in the coastal marine waters (Table 9). Compared to the

depleted values in the Newport River, the other estuarine NC δ^{13}C-DOM values were more enriched (Table 9). In TX, mean δ^{13}C-DOM values had the widest range between local ecosystems from -19.2‰ (tidal mudflat) to -27.3±5.89‰ (Aransas Pass; Table 9). The other two coastal waters sampled in TX had similar δ^{13}C-DOM values to the NC coastal marine sample (Table 11). As a whole site comparison, the tropical savanna climate of FL had significantly enriched δ^{13}C-DOM compared to NC ($p < 0.05$; Table 10). In FL, the range of δ^{13}C-DOM values was from -21.3±1.90‰ in the coastal waters around the Florida Keys to -25.0±1.06‰ in the mangrove pond on No Name Key (Table 9).

POM stable carbon isotopes (δ^{13}C-POM) were measured in four regions: NC, SC, TX, and FL (Fig. 5D). Compared to δ^{13}C-DOM values, δ^{13}C-POM values were significantly enriched as determined by an ANOVA on Ranks ($p < 0.05$). The most enriched δ^{13}C-POM values were found in FL followed by TX>NC>SC (Fig. 5D). The enriched δ^{13}C-POM values in FL were found in the coastal marine waters (-7.2‰) and waters around the Keys (-12.7±3.42‰). Even with the depleted δ^{13}C-POM values found in the mangrove pond on No Name Key (-25.1±0.01‰), an ANOVA on Ranks found FL values were significantly enriched compared to NC and SC values ($p < 0.05$; Table 12). The more depleted δ^{13}C-POM values in NC and SC were found primarily in the river estuarine systems (Table 11). Similar to FL coastal waters, TX also had enriched values in all of the sampling environments, with the exception of the urban canal, which was comparable to the river estuarine systems in NC and SC (Table 11).

Bulk elemental analysis of POM provided molar C:N ratios (Fig. 5F), with the majority of coastal waters in NC and FL having ratios >10, whereas in SC and TX the C:N

ratios were <10 (no data for HI; Table 11). The coastal waters in NC and FL had significantly higher ratios than coastal waters in SC, although only FL coastal waters were found to be significantly higher than TX (ANOVA on Ranks, $p < 0.05$; Table 12). The New River Estuary (15.64±4.52) in NC had the highest C:N ratios, which differed from the highest C:N ratio in FL, found in the coastal marine sample (24.31). The lowest ratios in NC and FL were from samples in Bogue Sound and the mangrove pond on No Name Key, respectively (Table 11). Similar to the environments with the highest and lowest C:N ratios in NC, the Cooper River Estuary (9.76±1.23) in SC had the highest C:N ratios, and the Charleston Harbor (7.26±0.23) had the lowest. Lastly in TX, the urban canal and channel adjacent to the tidal mudflat had the highest C:N ratios (9.25 and 9.24, respectively), and the coastal Gulf of Mexico at Aransas Pass had the lowest ratios (Table 11).

PARAFAC modeling of CDOM and BEPOM fluorescence

PARAFAC Model 1 was fit to 348 CDOM and 314 BEPOM EEM samples. The model was validated for six components (Fig. 7) using split-half validation to determine model efficiency, which was demonstrated through a comparison of the splits to modeled output (Fig. 8). Components derived from this model were queried to published PARAFAC models contained in the OpenFluor database (Murphy et al., 2014) with matches for all six components. Table 13 has the excitation and emission peak maxima for each component, which was matched to the peak nomenclature from Coble (1996). Component 1 (C1) was similar to terrestrial humic substances (Stedmon et al., 2007), and was identified as Peaks A and C (Table 13; Coble, 1996). Humic-like fluorescence at longer emission wavelengths is

generally from the degradation of terrestrial OM, typically originating in freshwater environments (Senesi, 1990; Coble et al., 2014), but has been found in environments such as a coastal lagoon, a freshwater wetland, and the continental shelf (Yamashita et al., 2010; Kowalczuk et al., 2013; Amaral et al., 2016). C2 exhibited fluorescence at shorter wavelengths than C1, which has been attributed to microbially reprocessed fulvic acids originating in terrestrial environments, although it has been found in a variety of coastal waters (Murphy et al., 2011; Stedmon et al., 2011). C3 is considered protein-like fluorescence because its excitation/emission (ex/em) properties resemble the amino acid tryptophan, which is indicative of active biological production (Coble et al., 2014). It has been found in environments such as sea ice, coastal seas, rivers and estuarine systems (Coble, 1996; Stedmon et al., 2011; Cawley et al., 2012; Osburn et al., 2012). C4 matched two published models that also performed BEPOM analysis (Osburn et al., 2012; Brym et al., 2014). In these previous studies, this component was found in estuaries and coastal waters with high nutrient loading that stimulate biological production within a system (Osburn et al., 2012; Brym et al., 2014). Similar to C1, C5 was attributed to terrestrial humic material; however, it exhibited a blue-shifted emission peak indicating degradation (Murphy et al., 2006; Coble, 2007; Osburn et al., 2011; Coble et al., 2014). Environments in which C5 has been found include lakes, ballast waters, and rivers (Murphy et al., 2006; Walker et al., 2009; Osburn et al., 2011). Component 6 (C6) shared similar ex/em peak characteristics to the amino acid tyrosine, and also is considered a “protein-like” component (Coble, 1996; Coble et al., 2014), typically found in areas with high primary production (Stedmon and Markager, 2005).

Model 1 components were explored to see which were dominant in CDOM and BEPOM size fractions, using each component's maximum fluorescent intensity (F_{max}) expressed as a percentage (Fig. 9A). Mean CDOM F_{max} distributions for all components were in similar proportions across all sites (Table 14). A minor deviation from this trend was observed in the humid subtropical climate of NC with C1 and C2 comprising approximately 68% of fluorescence because at the other sites C1 and C2 accounted for a range between 54 and 58% of total fluorescence (Fig. 9A; Table 14**)**. Overall, C2 was the most abundant component across all sites with percentages of 35±4%, 37±3%, 36±4%, 34±3%, and 33±7% in NC, SC, TX, FL, and HI, respectively (Table 14). The least abundant components in the CDOM samples varied among the study sites, including lesser abundance of C3 in NC and SC with percentages of 3±3% and 8±2%, respectively, while C4 was least abundant in TX at 8±1%. In contrast, C5 was least abundant in FL and HI with 7% abundances and SDs of ±2 and ±9, respectively (Table 14).

Compared to CDOM, where the relative distribution of the six components was similar across regions, the distribution of components present in BEPOM samples showed greater variability across sites (Fig. 9B). However, the dominant components in all regions were C3, C4, and C6. Specifically, C4 was most abundant in the BEPOM samples of the humid subtropical climates of NC (22±15%), SC (33±8%) and TX (41±17%). C6 was most abundant in the tropical rainforest climate of HI (35±4%; Table 15), whereas the tropical savanna climate of FL showed relatively similar abundances of C3, C4, and C6 (Table 15). In contrast to CDOM component distribution, BEPOM C1 and C2 were 2-6 times less prevalent in all regions (Tables 14 and 15). C1 was least abundant in NC (8±5%), TX (3±3%), and FL

(5±2%); while in SC, C5 was in lesser abundance (0%). However, C5 was also less abundant in FL BEPOM (5±5%; Table 15). Lastly, HI differed from the four other sites because C4 was the least abundant component (7±1%), and it was dominant in NC, SC, TX, and FL (Table 15).

A total of 342 CDOM fluorescence EEMs were compiled and a four-component model (Model 2) was created and validated as shown in Figure 10. Ex/Em spectra of each Model 2 component and model splits are shown in Figure 11, similar to Model 1. All four components matched published components on OpenFluor (Murphy et al., 2014). C1, C2, and C3 were identified as humic substances including terrestrial, degraded terrestrial and microbial fulvic acids, respectively. These three components have been found in a variety of environments such as open ocean waters in the equatorial, southern and northern Atlantic ocean and coastal waters from the Zambezi River, the Congo River, the San Francisco Bay, and three tropical rivers in Venezuela (Table 13; Senesi, 1990; Murphy et al., 2008; Williams et al., 2010; Yamashita et al., 2010; Jørgensen et al., 2011; Murphy et al., 2013; Lambert et al., 2016). C4 was associated with tryptophan protein fluorescence (Stedmon et al., 2007; Kowalczuk et al., 2009), which has been found in coastal waters with abundant allochthonous loadings from terrigenous and anthropogenic influences that increase the production within the systems (Stedmon et al., 2007; Yamashita et al., 2010; Bianchi et al., 2014; Shutova et al., 2014; Lambert et al., 2016).

Model 3 was fit to only BEPOM fluorescence samples with 313 EEMs, resulting in a split half validated 7-component model (Figs. 12 and 13). Query of Model 3 to the OpenFluor database resulted in matches for six of the seven components (Murphy et al.,

2014). C1 was identified as quinone-like material found in environments with higher rates of primary production such as eutrophic coastal waters (Osburn et al., 2012; Brym et al., 2014; Coble et al., 2014). C2 represented fluorescence patterns indicative of the amino acid, tryptophan (Murphy et al., 2006; Stedmon et al., 2007; Murphy et al., 2011) found in freshwater areas including Antarctic sea ice, the Gulf of Maine, and the Neuse River Estuary as well as the open Atlantic Ocean (Kowalczuk et al., 2009; Stedmon et al., 2011; Osburn et al., 2012; Cawley et al., 2012). C3 was identified as fresher terrestrial humic material compared to C4, which was described as degraded (Osburn et al., 2011; Shutova et al., 2014). Previous studies have identified C3 in many freshwater environments including the Neuse River Estuary, the Baltic Sea, the Japan Sea, and a subtropical lagoon (Stedmon et al., 2007; Brym et al., 2014; Tanaka et al., 2014; Amaral et al., 2016), although it has also been observed in eastern north Pacific waters (Catalá et al., 2015). C4 has been found in bodies of water such as a saline lake, an estuary, a river, and ballast waters (Murphy et al., 2006; Osburn et al., 2011; Murphy et al., 2013; Lambert et al., 2016). C5 represented microbially-reprocessed organic matter (Senesi, 1990; Coble et al., 2014) present in many different environments from freshwater to the open ocean including: sea ice, streams, rivers, ponds, estuarine systems, and the Pacific Ocean (Stedmon and Markager, 2005; Stedmon et al., 2007; Williams et al., 2010; Stedmon et al., 2011; Cawley et al., 2012; Tanaka et al., 2014; Catalá et al., 2015; Lambert et al., 2016). C6 showed tyrosine-like fluorescence common in areas with autochthonous production (Coble, 1996; Stedmon and Markager, 2005), and C7 was indicative of microbial humic material (Senesi, 1990; Brym et al., 2014) found in coastal environments (Stedmon et al., 2007; Stedmon et al., 2011; Amaral et al., 2016).

Tucker's Congruence Coefficient (TCC) analysis (Lorenzo-Seva and Berge, 2006) was conducted to compare similarity among the three PARAFAC model's components. Models 1 and 2 had no matches between components (Table 16). However, Models 1 and 3, components 1-6 in Model 3 matched six components from Model 2 (Table 17). C7 appeared to be a component unique to BEPOM because it was the only component, which did not match to a component from Model 1. Lastly, Models 2 and 3 were compared, and only one component (C2 – Model 2 and C3 – Model 3) matched between the two models (Table 18). Thus, the combined PARAFAC model was a better fit as compared to the BEPOM only model.

Overall the analysis of modeling CDOM and BEPOM together and separately argued strongly for use of a combined model. These results are consistent prior work, which has examined PARAFAC models of CDOM and BEPOM fit separately and combined (Osburn et al., 2012; Osburn et al., 2015). With this in mind, only the combined PARAFAC model will be discussed further.

DISCUSSION

The effect of antecedent weather conditions on OM quantity and quality

The hypothesis of this study was to determine if the Köppen climate classifications influenced DOM and POM quantity and quality, based on regional characteristics including mean air temperature and precipitation. A major finding from this research was that these long-term regional climate classifications were not indicative of the OM quantity or quality at the varying regions. Instead, local weather factors including antecedent precipitation, operating on 7-14 day timescales, along with the local surroundings (e.g., vegetation, proximity to OC source, and freshwater input), had greater impact on the OM quantity and quality observed in the geochemical measurements. Antecedent precipitation was defined as the total precipitation seven days prior to sampling (Table 1), and data for these local weather conditions was obtained from weather stations closest to the sampled coastal waters (when available) at each site. The coastal water endmembers (e.g., NC brackish marsh coastal waters, FL mangrove pond on No Name Key, TX tidal mudflat) at all five sites were excluded when interpreting the influence of antecedent conditions on DOM and POM (Fig. 16).

In all five regions, antecedent precipitation appeared to have a linear relationship to [DOC], although with greater variability during higher precipitation events, observed as higher standard deviations (Fig. 16A). NC and TX experienced heavier precipitation (>30 mm) than the three other sites prior to the samplings (Table 1). In NC these conditions likely increased flow and runoff from land to the rivers, thus potentially increasing [DOC] (Fig. 16A). Additionally, TX was experiencing a wet period from March 2015 to the end of

October 2015 with three major discharge events (average daily discharge of 8.7 m^3 s^{-1}) (Reyna et al., 2017) that likely contributed to the input of OM to the coastal waters through flushing events. Previous studies have supported that high flow events mobilize and increase OM concentrations from environments such as adjacent wetlands (Mladenov et al., 2005; Hood et al., 2006; Eimers et al., 2008; Tzortziou et al., 2008) and terrestrial ecosystems (Dalzell et al., 2007), supporting the claim that an increase in DOM quantity could be attributed to heavier precipitation. Thus, local precipitation weather events, rather than regional climate classifications, seemed to influence to a greater extent the DOM concentrations in these field areas.

Trends in DOM quality were also explored against antecedent precipitation. Generally, δ^{13}C-DOM values decreased with higher precipitation, whereas $SUVA_{254}$ values increased with more precipitation (Figs. 16C and 16E). For example, FL δ^{13}C-DOM values were slightly more enriched than the other sites, approximately ranging from -18 to -24‰, whereas the $SUVA_{254}$ values in FL were lower than the other sites (Figs. 16C and 16E), with the exception of TX. These results suggest autochthonous influences in the FL coastal waters (Lamb et al., 2006; Jaffé et al., 2008). In contrast to FL, the greater allochthonous DOM quality in NC shown in the significantly more depleted δ^{13}C-DOM values ($p < 0.05$; Table 10) and higher $SUVA_{254}$ values (Jaffé et al., 2008; Bianchi and Bauer, 2011) was likely the result of heavier antecedent precipitation. The impact of antecedent precipitation on DOM quality in this study is similar to a study that analyzed three watersheds before and after storm events (Hood et al., 2006). The terrestrial influence on the DOM quality was observed in the watersheds after these storm events through higher $SUVA_{254}$ values (Hood et al.,

2006). Thus, similar to DOM quantity, DOM quality was also affected by antecedent precipitation.

The influence of antecedent precipitation on POM quality was shown in the trends with δ^{13}C-POM values and C:N ratios (Figs. 16D and 16F). Similar to δ^{13}C-DOM values (Fig. 16C), δ^{13}C-POM values were more depleted (approximately -18 to -25‰) in the three sites (NC, SC, and TX) with heavier precipitation (Table 1, Fig. 16D). Specifically in NC and SC, the depleted δ^{13}C-POM values (-25 to -33‰; Fig. 6) suggested allochthonous sources, including C3 vascular plants and soil-derived OM (Lamb et al., 2006). However, the NC and SC coastal waters differed in the ranges of C:N ratios (Table 11, Fig. 6), with significantly higher C:N ratios in NC (mean: 12.06±3.07) than SC (mean: 8.86±1.25; $p < 0.05$; Table 12). Typically, C:N ratios >12 are associated with allochthonous sources such as terrestrial vegetation, whereas C:N ratios <10 are indicative of autochthonous POM (Lamb et al., 2006). Thus, it appears that allochthonous OM was more prevalent in NC POM than SC likely from the higher precipitation prior to sampling (Figs. 16D and 16F). These POM results were similar to the findings for DOM quality in three small Oregon watersheds in which there was a terrestrial influence associated with storm events (Hood et al., 2006). Together these suggested that, similar to DOM, local weather exerted more control on the POM quality than the Köppen climate classifications.

DOM quantity differences and POM quantity similarities across sites

DOM quantity in coastal waters was expected to vary based on the Köppen climate classifications, however there were no significant differences in the CDOM-DOC

relationship in four of the five sites (NC, SC, FL, and HI; Table 6). TX was the exception and had a relative ratio of a_{254}d values to [DOC] that was significantly lower than the other four regions (Table 6, Fig. 2), suggesting less CDOM relative to [DOC] in the TX coastal waters. Photodegradation is a likely explanation for a loss of CDOM without affecting the [DOC] (Waiser and Robarts, 2004; Maie et al., 2006; Osburn et al. 2009), supported by the low $SUVA_{254}$ values and high S_Rd values (Table 9) that have been associated with photochemical processes (Helms et al., 2008; Spencer et al., 2009; Zhang et al., 2009). Low $SUVA_{254}$ values indicate less aromatic DOM, which would be consistent with high S_Rd values that indicate low molecular weight OM (Helms et al., 2008). In comparison to the TX semi-arid coastal waters, a previous study found high S_Rd values in the surface waters of tropical and open ocean environments primarily due to photobleaching of DOM (Yamashita et al., 2013). Therefore, CDOM results indicated that the relative amount of CDOM to [DOC] differed only in TX compared to the four other regions, therefore implying the importance of local environmental conditions (e.g., sunlight and surface water residence time) on DOM concentrations. In contrast to the primary effect of local weather such as antecedent precipitation, secondary effects such as residence time may modulate DOM quality, an effect that may be attributable to regional climate.

Additionally, DOM quantity (a_{254}d values and [DOC]) seemed to be influenced by the proximity of the coastal waters to OM sources. For instance, coastal waters in NC, SC, TX, and FL closest to freshwater or endmembers, such as rivers or adjacent wetlands, had the highest DOM concentrations, whereas the coastal marine waters closer to the continental shelf in these sites had the lowest concentrations (Table 3). Specifically in NC, the DOM

concentrations found in the Newport River and brackish marsh coastal waters were highest compared to other coastal waters in this region (Table 3). Similarly, the TX tidal mudflat, isolated from the other coastal waters, had the highest $a_{254}d$ value and [DOC] (Table 3). The high concentrations in these coastal waters were likely the result of the close proximity to land and the marsh environment that would have been more susceptible to runoff from the heavy antecedent precipitation (Table 1), and are comparable to higher [DOC] from a study that examined DOM and POM before and after a hurricane in the Neuse River Estuary (Osburn et al., 2012). Before and after the storm event, the estuarine station closest to the river had the highest [DOC] in comparison to the station closer to the estuary proper (Osburn et al., 2012). The findings from this study along with Osburn et al. (2012) indicate that DOM concentrations were directly linked to proximity to OM sources.

POM quantity ($a_{254}p$ values and [POC]) had similar concentrations across the five sites. Few significant differences in $a_{254}p$ values and [POC] ($p < 0.05$; Table 4) were observed, supporting the similarity in POM quantity among regions. Additionally, PCA scores along PC1 (49.72%), which seemed to be partially influenced by a_{254} values and OC concentrations (Figs. 15A), showed that BEPOM samples had a smaller range than CDOM samples (Fig. 15B). These PCA scores further emphasized the lower variability in POM concentrations than DOM quantity across sites. Although results from this study suggest similarity in POM quantity, Bianchi and Bauer (2011) describe the distribution of [POC] in coastal waters as varying on the chemical and physical processes in estuaries and coastal waters (e.g., OM reactivity, salinity, re-suspension, sinking) that emphasize the dependency

on local environment. Overall, POM concentrations in the five studied sites were less influenced by Köppen climate classifications than by local antecedent weather conditions.

DOM quality similarity and POM quality variability among sites

Within the context of regional climate, one major finding of this study was that DOM quality was generally similar among the sites studied. For example, there were few instances of significant differences in $SUVA_{254}$ values, no significant differences in S_Rd values, only one significant difference in δ^{13}C-DOM values among sites ($p < 0.05$; Table 10), and similar PARAFAC Model 1 component distribution in CDOM samples (Table 14, Fig. 9A). The minimal significant differences in $SUVA_{254}$ values suggest similar DOM aromaticity, and the lack of differences in S_Rd values indicate comparable ranges in DOM molecular weight in these coastal regions (Tables 9 and 10, Fig. 5A). Additionally, the range of δ^{13}C-DOM values in NC, TX, and FL was small with approximate values of -26‰, -23‰, and -22‰, respectively that indicates similarity of DOM sources among these three sites (Fig. 5C). Lastly, the distribution in CDOM fluorescence included similar relative abundances of PARAFAC components across the five sites (Table 13, Fig. 9A). The greatest abundances of C1 and C2 (Table 14) and ubiquitous nature of these terrestrial humic- (C1) and microbial humic- (C2) like components found in this study and previous studies (Osburn et al., 2015; Ya et al., 2015) also suggest that DOM sources to surface coastal waters are similar. The similarity in the DOM quality across these diverse coastal regions suggests that processes controlling DOM lead to homogenization of the DOM pool. This likely occurs from similar

re-working or processing of OM before entering the coastal waters (regardless of region), and fewer modifications as DOM is transported to the coastal ocean.

POM quality differed from DOM quality in lability (fresh or degraded) and sources of OM (humic vs. planktonic). The separation between positive and negative PARAFAC component loadings over PC2 (20.30%) seemed to be associated with degraded and fresh OM, respectively (Fig. 15A). For instance, C5 has previously been linked to degraded terrestrial material because of its blue-shifted emission peak (Murphy et al., 2006; Coble, 2007; Coble et al., 2014). C6, which exhibited similar ex/em characteristics to tyrosine (Coble, 1996; Coble et al., 2014), is also likely indicative of degradation because of the degraded peptides in tyrosine (Fellman et al., 2008). Due to the greater range of BEPOM scores over PC2 compared to CDOM scores, BEPOM samples appeared to be more variable in lability. Additionally, separation along PC1 (49.72%) appeared to differentiate humic (C1, C2, and C5) vs. planktonic (C3, C4, and C6) PARAFAC components. The majority of CDOM sample scores plotted closer to the humic components, whereas the BEPOM samples clustered towards the planktonic components (Fig. 15B). The separation between the two size fractions based on lability and source was also found in a study that used PARAFAC to analyze OM quality between DOM and POM in the tidal creek of a salt marsh adjacent to the North River estuary in NC (Osburn et al., 2015). Thus, leading to the conclusion that DOM seemed to be minimally influenced once input into the coastal waters, supporting the allochthonous quality. In contrast, the POM quality appeared to be directly impacted by in situ processes and autochthonous sources, while also ranging in fresh or degraded quality.

Local vegetation also exerted a major control on the POM quality. For example, the POM quality in the FL coastal waters showed the influence of seagrass. Seagrass has been found to be abundant within Florida Bay, which is slightly north of sites sampled, although regionally in the same area (Ya et al., 2015). Although a seagrass signature was not as noticeable in the FL DOM, it was more evident in the FL POM quality through enriched δ^{13}C-POM values (-7.2 to -12.7±3.42‰) and high C:N ratios (14.25 to 24.31) (Table 11, Figs. 6, 16D, 16F). The relationship between δ^{13}C-POM values and C:N ratios suggests an influence from C4 plants (Lamb et al., 2006), likely seagrass due to the similarity in the mean δ^{13}C-POM value (-8.7±0.04‰) and mean C:N ratio (26.14±1.31) of the seagrass endmember collected from the studied FL coastal waters (Fig. 6). In contrast to FL, the Newport River and brackish marsh in NC showed the impact of allochthonous vegetation through the C:N ratios >12 and δ^{13}C-POM values (-27.9±1.46‰ and -26.4‰, respectively). The δ^{13}C-POM values reflect ranges observed for sources such as terrigenous OM (e.g., vascular plants: -26 to -30‰, soils: -23 to -27‰) and marsh OM (e.g., C3 brackish marsh plants: -23 to -26‰) (Bianchi, 2006). Lastly, the enriched δ^{13}C-POM value (-14.8‰) and C:N ratio (8.72) in the TX tidal mudflat, covered in sparse mangrove vegetation, are likely due to some combination of C4 plant material (-9 to -17‰) and microbial reprocessed soil OM (Kendall et al., 2001). The TX tidal mudflat showed more of an indirect influence from vegetation than the other sites likely due to flushing event (Reyna et al., 2017) that input OM to this isolated system, thus potentially increasing the microbial activity. Overall, these results emphasize the importance of local vegetation on POM quality, as well as the linkage to other local environmental factors (e.g., antecedent weather and in situ processes).

CONCLUSIONS

The aim of this study was to examine OM quantity and quality in five coastal and estuarine systems under varying climatic conditions. The study sites included: the Lower Outer Banks, NC; Charleston Harbor, SC; Corpus Christi Bay and Aransas Pass, TX; Florida Keys near Key West, FL; and Kahana Bay, HI. A variety of coastal waters ranging from tidal rivers to inner continental shelf waters were sampled within each region. Abundance measurements such as CDOM and BEPOM a_{254} values along with [DOC] and [POC] were used to characterize the relative amount of OC transported from land to the coastal ocean in these five environments. Absorbance and fluorescence spectroscopy, stable carbon isotopic analysis, and bulk elemental ratios were used as indicators of quality and source of the OM. Fluorescence measurements were modeled using PARAFAC analysis, and a PCA was performed to identify main controls on the variation of the data and to elucidate general trends in the two OM pools.

The major finding from this research was that the Köppen climate classifications were not the main forcing factor for OM quantity or quality. Instead the local environments (e.g., vegetation, proximity to OC source, and freshwater input) coupled with local weather factors (e.g., precipitation, air temperature, storm events) had the most direct impact on OM. These effects were most evident in POM quality and not DOM. Another finding from this research was the variability in DOM quantity and similarity in POM quantity in the five regions. The range in DOM concentrations was higher than the range observed in the POM concentrations (Fig. 1), however neither DOM nor POM abundances seemed to be controlled by the Köppen climate classifications. Lastly, DOM quality was generally similar in the five regions,

whereas POM quality appeared to be driven by antecedent conditions and vegetation. DOM quality similarities suggest that there are similar processes controlling DOM across these coastal environments, which lead to uniformity within the DOM pool regardless of climatic region. In contrast, POM quality appeared to be directly linked to the local environment, which led to its higher variability as well as its predominant autochthonous signature. The results from this study suggest further investigation into the effects of these local environments on OM dynamics as well as the extent to which they would impact OM contributions to the global carbon cycle. Also, it would be beneficial to understand the implications associated with changes to these coastal environments and the respective OM contributions from these changes.

Future work should include longer temporal and greater spatial scales in order to better evaluate if weather/climatic conditions have an effect on regional OM dynamics. This study suggests that local conditions and weather factors dictated the OM quantity and quality across the five studied regions. However, sampling over a longer or continuous time scale would aid in determining if long-term climate classifications were actually forcing OM dynamics (e.g., quantity and quality). For example, a previous study found that a local storm event (e.g., hurricane) disrupted OM dynamics in a river-dominated NC estuary (Osburn et al., 2012). However, with a longer sampling period, it is likely that the effect of a local event would be minimal on OM quantity and quality. Extensive seasonal sampling would help clarify the dependency of OM dynamics on local weather conditions, such as storms or heavy precipitation events. Additionally, characterizing OC fluxes on a seasonal basis could be used to determine better estimates of the amount of OM transported to the coastal oceans.

This study has aided in closing knowledge gaps about OM dynamics in coastal systems with regards to variability in quantity and quality. Many coastal waters produce, transform, and degrade OC during transport to more open-ocean environments (Cai, 2011; Bauer et al., 2013). However, with sea level rise resulting from global climate change there are ramifications that would affect organic carbon dynamics in coastal waters and ecosystems, mainly through losses of habitats and coastal wetlands (Nicholls, 2004; McLeod et al., 2011). Consequently, these impacted systems are very important to study. Moreover, this research will complement local and regional carbon budgets, having direct connections to global carbon and climate change policy. For example, the Intergovernmental Panel on Climate Change (IPCC) could use some of these data in their synthesis reports (IPCC, 2014), and specifically for their assessment reports on carbon and other biogeochemical cycles (Ciais et al., 2014). This research has built on prior multi-system OM biogeochemical research in the following ways: incorporation of additional analyses; observations of both dissolved and particulate OM; sample collection in varying coastal waters from freshwater areas (e.g., rivers) to brackish/marine environments (e.g., brackish marsh, estuaries, mangroves, seagrass); and contrasting regional sampling locations (Jaffe et al., 2008; Spencer et al., 2012; Ya et al., 2015; Osburn et al., 2016).

TABLES

Table 1. Mean air temperatures (°C) and total precipitation (mm) seven days prior to sampling and during sampling. Data compiled using daily averages from National Climatic Data Center (https://www.ncdc.noaa.gov/cdo-web/).

Region	Date	Temp. Prior (°C)	Precip. Prior (mm)	Temp. During (°C)	Precip. During (mm)
NC	Apr 2014	17.7	19.1	8.3	0
	Aug 2014	25.0	145.0	25.4	44.2
	Nov 2014	14.3	44.5	6.5	8.4
	Aug 2015	25.3	53.8	24.9	46.7
SC	Jun 2011	29.6	13.5	26.9	0.3
TX	Sep 2015	27.4	51.3	29.4	0
FL	May 2013	25.5	0	26.0	0.5
	Aug 2013	29.5	0.5	27.5	6.9
	Nov 2013	26.6	0	24.2	0
	Oct 2015	27.1	7.4	27.8	0
HI	Jul 2010	23.2	8.1	22.8	4.3
	Aug 2011	23.4	14.5	23.3	0.8

Table 2. Mean annual air temperatures (°C) and mean annual precipitation (mm) for years sampled, latitudes (°N), and Köppen climate classifications.

Region / Sampling years	Temp. (°C)	Precip. (mm)	Latitude (°N)	Climate Classification
NC 2014	17.01	113.77	34° 43’ 40’’	Humid Subtropical
2015	17.88	170.46		
SC 2011	19.90	66.77	32° 47’ 00’’	Humid Subtropical
TX 2015	22.38	104.68	27° 46’ 20’’	Humid Subtropical
FL 2013	25.91	98.88	24° 33’ 33’’	Tropical Savanna
2015	26.61	76.79		
HI 2010	22.55	98.14	21° 33’23’’	Tropical Rainforest
2011	23.19	137.58		

Table 3. DOM and POM concentration measurements (mean ± standard deviation) and sampling area description within each site. 'N.D.' indicates no data. Numbers in parentheses denote number of samples measured for each type of analysis.

Region / Locations	$a_{254}d$ (m^{-1})	[DOC] (mg L^{-1})	$a_{254}p$ (m^{-1})	[POC] (mg L^{-1})	Description
NC					
Newport River	349.28±78.97 (4)	31.8±8.40 (4)	6.63±3.04 (4)	2.0±0.59 (4)	River and cypress bog
Newport River Estuary	112.72±97.21 (26)	15.5±10.49 (26)	1.65±1.83 (26)	1.7±0.87 (26)	Estuary
Bogue Sound	35.43±48.70 (10)	3.2±0.57 (6)	0.59±0.53 (10)	1.0±0.71 (9)	Estuary
White Oak River Estuary	28.96±9.56 (8)	7.3±2.84 (8)	0.90±0.98 (8)	1.8±1.45 (8)	Estuary
New River Estuary	67.27±36.67 (10)	8.4±3.36 (10)	4.21±3.13 (10)	4.4±2.25 (10)	Estuary
Marsh	268.19 (1)	27.2 (1)	5.05 (1)	2.4 (1)	Brackish marsh
Coastal Marine	2.66 (1)	7.2 (1)	0.12 (1)	0.2 (1)	Coastal ocean
SC					
Cooper River Estuary	18.52±2.91 (8)	3.5±0.92 (9)	0.40±0.20 (11)*	1.0±0.30 (9)	Estuary
Ashley River Estuary	25.86±0.10 (2)	3.3±0.02 (2)	0.50±0.12 (2)*	1.3±0.03 (2)	Estuary
Wando River Estuary	16.11±2.17 (3)	2.4±0.56 (4)	0.94±0.98 (4)*	0.9±0.14 (3)	Estuary
Charleston Harbor	18.99±2.93 (3)	2.6±0.34 (3)	0.29±0.03 (3)*	0.8±0.06 (3)	Estuary
Coastal Marine	3.62±0.65 (3)	1.1±0.16 (3)	0.14±0.02 (3)*	0.3±0.04 (3)	Coastal ocean
TX					
Urban canal	58.17 (1)	18.7 (1)	4.35 (1)	5.3 (1)	River
Tidal Mudflat	72.48 (1)	42.7 (1)	2.81 (1)	3.2 (1)	Tidal flat
Channel near tidal mudflat	13.74 (1)	13.3 (1)	0.45 (1)	0.8 (1)	Channel
Aransas Pass	8.65±2.21 (2)	14.9±5.63 (2)	0.34±0.04 (2)	0.9±0.27 (2)	Coastal ocean
FL					
Channels around Florida Keys	5.94±3.26 (28)	1.8±0.57 (28)	0.13±0.02 (20)	0.5±0.59 (11)	Coastal ocean
No Name Key mangrove pond	125.65±16.72 (3)	15.0±1.65 (3)	1.59±1.71 (3)	3.5±3.47 (2)	Mangrove pond
Coastal Marine	5.09±0.65 (2)	1.4±0.15 (2)	0.08±0.01 (2)	0.7 (1)	Coastal ocean
HI					
Kahana Bay	4.83±1.95 (14)	1.4±0.41 (13)	0.49±0.30 (9)	N.D.	Estuary

*Values taken from Brym et al., 2014

Table 4. Summary of ANOVA on Ranks followed by Dunn's Test to determine significant differences and to identify which sites were significantly different for quantitative measurements of DOM and POM. 'Yes' indicates significant difference ($p < 0.05$), 'No' indicates no significant difference ($p > 0.05$), and 'N.D.' denotes no data.

		Region						Region				
	a_{254}d	NC	SC	TX	FL	HI	**a_{254}p**	NC	SC	TX	FL	HI
Region	NC		**Yes**	No	**Yes**	**Yes**			**Yes**	No	**Yes**	No
	SC			No	No	No				No	No	No
	TX				No	No					**Yes**	No
	FL					No						No
	HI											
	[DOC]						**[POC]**					
Region	NC		**Yes**	No	**Yes**	**Yes**			**Yes**	No	**Yes**	N.D.
	SC			**Yes**	No	No				No	No	N.D.
	TX				**Yes**	**Yes**					No	N.D.
	FL					No						N.D.
	HI											

Table 5. Results of a linear regression model fit to each region's $a_{254}d$ vs. [DOC] results: $a_{254}d = m \times [DOC] + b$, where m is slope and b is intercept. $p < 0.05$ indicates statistically significant slope of $a_{254}d$ vs. [DOC].

Region	m(±SE)	b(±SE)	r^2	p
NC	8.780±0.83	-12.561±14.07	0.698	<0.001
SC	4.874±0.92	3.117±2.73	0.639	<0.001
TX	2.094±0.34	-19.074±8.45	0.950	<0.05
FL	9.028±0.14	-10.562±0.79	0.995	<0.001
HI	3.810±0.74	-0.357±0.96	0.726	<0.001

Table 6. Summary of ANCOVA results with Tukey's post-test to identify sites with significantly different [DOC] vs. a_{254}d slopes from Figure 2. 'Yes' indicates significant difference ($p < 0.05$) and 'No' indicates no significant difference ($p > 0.05$).

		Region				
	[DOC] vs. a_{254}d	NC	SC	TX	FL	HI
Region	NC		No	**Yes**	No	No
	SC			**Yes**	No	No
	TX				**Yes**	**Yes**
	FL					No
	HI					

Table 7. Results of a linear regression model fit to each region's seasonal $a_{254}d$ vs. [DOC] results: $a_{254}d = m \times [DOC] + b$, where m is slope and b is intercept. $p < 0.001$ and $p < 0.05$ indicate statistically significant slope of $a_{254}d$ vs. [DOC]. 'N.S.' indicates not statistically significant. FL November 2013 sampling only had two samples therefore a regression was not fit.

Region	Date	m(±SE)	b(±SE)	r^2	p
NC	Apr 2014	-0.363±2.83	61.873±22.19	-	N.S.
	Aug 2014	11.849±0.44	-11.303±9.12	0.988	<0.001
	Nov 2014	12.940±0.74	-21.951±8.60	0.974	<0.001
	Aug 2015	8.910±1.14	-72.630±24.64	0.804	<0.001
SC	Jun 2011	4.874±0.92	-3.117±2.73	0.639	<0.001
TX	Sep 2015	2.094±0.34	-19.074±8.45	0.950	<0.05
FL	May 2013	2.886±1.06	2.472±2.41	-	N.S.
	Aug 2013	8.685±0.18	-9.799±0.98	0.997	<0.001
	Nov 2013	-	-	-	-
	Oct 2015	8.943±0.28	-9.814±1.46	0.995	<0.001
HI	Jul 2010	4.336±0.61	-1.559±0.84	0.926	<0.05
	Aug 2011	4.592±0.21	-0.793±0.30	0.990	<0.001

Table 8. Summary of ANCOVA results with Tukey's post-test to identify sites with significantly different [DOC] vs. $a_{254}d$ slopes for seasonal samplings shown in Figure 2. 'Yes' indicates significant difference ($p < 0.05$) and 'No' indicates no significant difference ($p > 0.05$).

[DOC] vs. $a_{254}d$	**Region**	Date				**Region**	Date	
	NC	Apr 14	Aug 14	Nov 14	Aug 15	**HI**	Jul 10	Aug 11
Date	Apr 14		No	No	**Yes**	Jul 10		No
	Aug 14			No	**Yes**	Aug 11		
	Nov 14				**Yes**			
	Aug 15							
	FL	May 13	Aug 13	Nov 13	Oct 15			
Date	May 13		No	No	No			
	Aug 13			No	No			
	Nov 13				No			
	Oct 15							

Table 9. Qualitative measurements (mean ± standard deviation) for DOM across five sites. 'N.D.' denotes no data. Numbers in parentheses denote number of samples measured for each type of analysis.

Region / Locations	S_Rd	δ^{13}C-DOM (‰)	CDOM $SUVA_{254}$ (L mg C^{-1} m^{-1})
NC			
Newport River	0.74±0.04 (4)	-27.1±1.70 (4)	4.92±1.03 (4)
Newport River Estuary	0.95±0.28 (26)	-26.5±1.76 (24)	3.20±1.44 (24)
Bogue Sound	1.08±0.16 (10)	-26.1±1.99 (8)	3.44±0.82 (7)
White Oak River Estuary	0.97±0.04 (8)	-25.2±2.01 (8)	2.11±1.29 (8)
New River Estuary	0.89±0.14 (10)	-26.6±0.51 (10)	3.06±1.29 (10)
Marsh	0.80 (1)	-25.3 (1)	4.29 (1)
Coastal Marine	1.82 (1)	-22.6 (1)	0.16 (1)
SC			
Cooper River Estuary	1.17±0.12 (10)	N.D.	2.25±0.33 (8)
Ashley River Estuary	1.07±0 (2)	N.D.	3.45±0.01 (2)
Wando River Estuary	1.17±0.07 (4)	N.D.	3.13±0.17 (3)
Charleston Harbor	1.12±0.03 (3)	N.D.	3.19±0.20 (3)
Coastal Marine	1.39±0 (2)	N.D.	1.41±0.08 (3)
TX			
Urban canal	1.01 (1)	-23.6 (1)	1.35 (1)
Tidal Mudflat	1.17 (1)	-19.2 (1)	0.74 (1)
Channel near tidal mudflat	1.25 (1)	-22.7 (1)	0.45 (1)
Aransas Pass	1.61±0.56 (2)	-27.3±5.89 (2)	0.26±0.03 (2)
FL			
Channels around Florida Keys	1.17±0.37 (27)	-21.3±1.90 (19)	1.18±0.55 (19)
No Name Key mangrove pond	1.12±0.06 (3)	-25.0±1.06 (3)	3.63±0.14 (3)
Coastal Marine	1.22±0.05 (2)	-23.0±1.80 (2)	1.60±0.03 (2)
HI			
Kahana Bay	0.95±0.36 (13)	N.D.	1.55±0.24 (13)

Table 10. Summary of ANOVA on Ranks followed by Dunn's Test to determine significant differences for qualitative properties of DOM. 'Yes' indicates significant difference ($p < 0.05$), 'No' indicates no significant difference ($p > 0.05$), and 'N.D.' denotes no data.

		Region				
	S_Rd	NC	SC	TX	FL	HI
Region	NC		No	No	No	No
	SC			No	No	No
	TX				No	No
	FL					No
	HI					
	δ^{13}C-DOM					
Region	NC		N.D	No	**Yes**	N.D.
	SC			N.D.	N.D.	N.D.
	TX				No	N.D.
	FL					N.D.
	HI					
	CDOM $SUVA_{254}$					
Region	NC		No	**Yes**	No	No
	SC			**Yes**	**Yes**	No
	TX				No	No
	FL					No
	HI					

Table 11. Qualitative measurements (mean ± standard deviation) for POM across five sites. 'N.D.' denotes no data. Number in parentheses denotes number of samples measured for each type of analysis.

Region / Locations	S_Rp	δ^{13}C-POM (‰)	POM C:N
NC			
Newport River	0.87±0.02 (4)	-27.9±1.46 (4)	14.92±3.45 (4)
Newport River Estuary	2.21±1.08 (26)	-24.7±2.15 (26)	11.29±2.35 (26)
Bogue Sound	3.04±0.82 (10)	-21.6±1.80 (9)	10.19±0.96 (9)
White Oak River Estuary	2.62±0.80 (8)	-20.0±4.05 (8)	11.08±1.35 (8)
New River Estuary	2.34±0.56 (10)	-20.2±2.85 (10)	15.64±4.52 (10)
Marsh	0.94 (1)	-26.4 (1)	14.01 (1)
Coastal Marine	4.63 (1)	-21.4 (1)	11.33 (1)
SC			
Cooper River Estuary	N.D.	-24.5±2.30 (9)	9.76±1.23 (9)
Ashley River Estuary	N.D.	-22.6±0.00 (2)	8.72±0.16 (2)
Wando River Estuary	N.D.	-21.9±0.54 (3)	8.43±0.34 (3)
Charleston Harbor	N.D.	-22.6±0.24 (3)	7.26±0.23 (3)
Coastal Marine	N.D.	-25.3±0.38 (3)	8.31±0.65 (3)
TX			
Urban canal	4.93 (1)	-25.1 (1)	9.25 (1)
Tidal Mudflat	1.82 (1)	-14.8 (1)	8.72 (1)
Channel near tidal mudflat	2.99 (1)	-17.6 (1)	9.24 (1)
Aransas Pass	3.96±0.63 (2)	-19.6±0.66 (2)	8.26±3.55 (2)
FL			
Channels around Florida Keys	3.93±2.43 (17)	-12.7±3.42 (11)	14.25±2.87 (11)
No Name Key mangrove pond	3.57±0.82 (3)	-25.1±0.01 (2)	9.44±0.93 (2)
Coastal Marine	2.55 (1)	-7.2 (1)	24.31 (1)
HI			
Kahana Bay	1.93±0.90 (9)	N.D.	N.D.

Table 12. Summary of ANOVA on Ranks followed by Dunn's Test to determine significant differences for qualitative properties of POM. 'Yes' indicates significant difference ($p < 0.05$), 'No' indicates no significant difference ($p > 0.05$), and 'N.D.' denotes no data.

		Region				
	S_Rp	NC	SC	TX	FL	HI
Region	NC		N.D.	No	No	No
	SC			N.D.	N.D.	N.D.
	TX				No	No
	FL					No
	HI					
	δ^{13}C-POM					
Region	NC		No	No	**Yes**	N.D.
	SC			No	**Yes**	N.D.
	TX				No	N.D.
	FL					N.D.
	HI					
	POM C:N					
Region	NC		**Yes**	No	No	N.D.
	SC			No	**Yes**	N.D.
	TX				**Yes**	N.D.
	FL					N.D.
	HI					

Table 13. Component excitation and emission maxima from PARAFAC Models 1 (CDOM and BEPOM), 2 (CDOM) and 3 (BEPOM) along with number of component matches on OpenFluor database, and a description of each component.

Model	Comp.	Ex_{max}	Em_{max}	Matches	Coble Peaks	Description
1	C1	240	496	21	A+C	Terrestrial humic
	C2	240 (310)	404	27	M	Microbial humic
	C3	270	342	10	T	Tryptophan protein
	C4	255 (370)	450	2		Quinone-like
	C5	240	432	6	A	Degraded terrestrial humic
	C6	275*	310*	0		Unidentified
2	C1	240	436	7		Terrestrial humic
	C2	240 (375)	506	17	A+C	Terrestrial humic
	C3	240 (300)	380	4	M	Microbial humic
	C4	275	332	15	T	Tryptophan protein
3	C1	255 (365)	450	2		Quinone-like
	C2	270	346	11	T	Tryptophan protein
	C3	240	510	20	A+C	Terrestrial humic
	C4	240	432	4	A	Degraded terrestrial humic
	C5	240 (320)	404	24	M	Microbial humic
	C6	275*	310*	0		Unidentified
	C7	240 (300)	344	9		Microbial humic

*Approximate Ex. and Em. maxima

Table 14. Mean (±SD) of F_{max} percentages for PARAFAC Model 1 component distribution for only CDOM samples across regional climate classifications.

	Location and climate region				
Component	**NC - humid subtropical (%)**	**SC - humid subtropical (%)**	**TX - humid subtropical (%)**	**FL - tropical savanna (%)**	**HI - tropical rainforest (%)**
C1	33±8	21±2	19±3	20±3	22±7
C2	35±4	37±3	36±4	34±3	33±7
C3	3±3	8±2	11±2	12±3	11±9
C4	10±2	11±1	8±1	9±1	9±5
C5	12±4	9±2	13±3	7±2	7±9
C6	7±4	13±6	13±5	17±4	18±12

Table 15. Mean (±SD) of F_{max} percentages for Model 1 component distribution for only BEPOM samples across regional climate classifications.

	Location and climate region				
Component	**NC - humid subtropical (%)**	**SC - humid subtropical (%)**	**TX - humid subtropical (%)**	**FL - tropical savanna (%)**	**HI - tropical rainforest (%)**
C1	8±5	12±5	3±3	5±2	8±2
C2	9±5	15±6	4±2	8±3	13±5
C3	15±9	24±7	22±9	25±6	21±9
C4	22±15	33±8	41±17	28±10	7±1
C5	16±15	0	4±5	5±5	15±10
C6	31±10	16±5	27±9	29±8	35±4

Table 16. Matrix of match results using TCC analysis between Model 1 (CDOM and BEPOM) and Model 2 (CDOM only). Ones indicate both ex/em loadings congruence coefficients (r_c) > 0.95, denoting similarity between components.

	Model 2			
Model 1	**C1**	**C2**	**C3**	**C4**
C1	0	0	0	0
C2	0	0	0	0
C3	0	0	0	0
C4	0	0	0	0
C5	0	0	0	0
C6	0	0	0	0

Table 17. Matrix of match results using TCC analysis between Model 1 (CDOM and BEPOM) and Model 3 (BEPOM only). Ones indicate ex/em loadings congruence coefficients (r_c) > 0.95, denoting similarity between components.

	Model 3						
Model 1	**C1**	**C2**	**C3**	**C4**	**C5**	**C6**	**C7**
C1	0	0	**1**	0	0	0	0
C2	0	0	0	0	**1**	0	0
C3	0	**1**	0	0	0	0	0
C4	**1**	0	0	0	0	0	0
C5	0	0	0	**1**	0	0	0
C6	0	0	0	0	0	**1**	0

Table 18. Matrix match results using TCC analysis between Model 2 (CDOM only) and Model 3 (BEPOM only). Ones indicate ex/em loadings congruence coefficients (r_c) > 0.95, denoting similarity between components.

	Model 3						
Model 2	**C1**	**C2**	**C3**	**C4**	**C5**	**C6**	**C7**
C1	0	0	0	0	0	0	0
C2	0	0	**1**	0	0	0	0
C3	0	0	0	0	0	0	0
C4	0	0	0	0	0	0	0

FIGURES

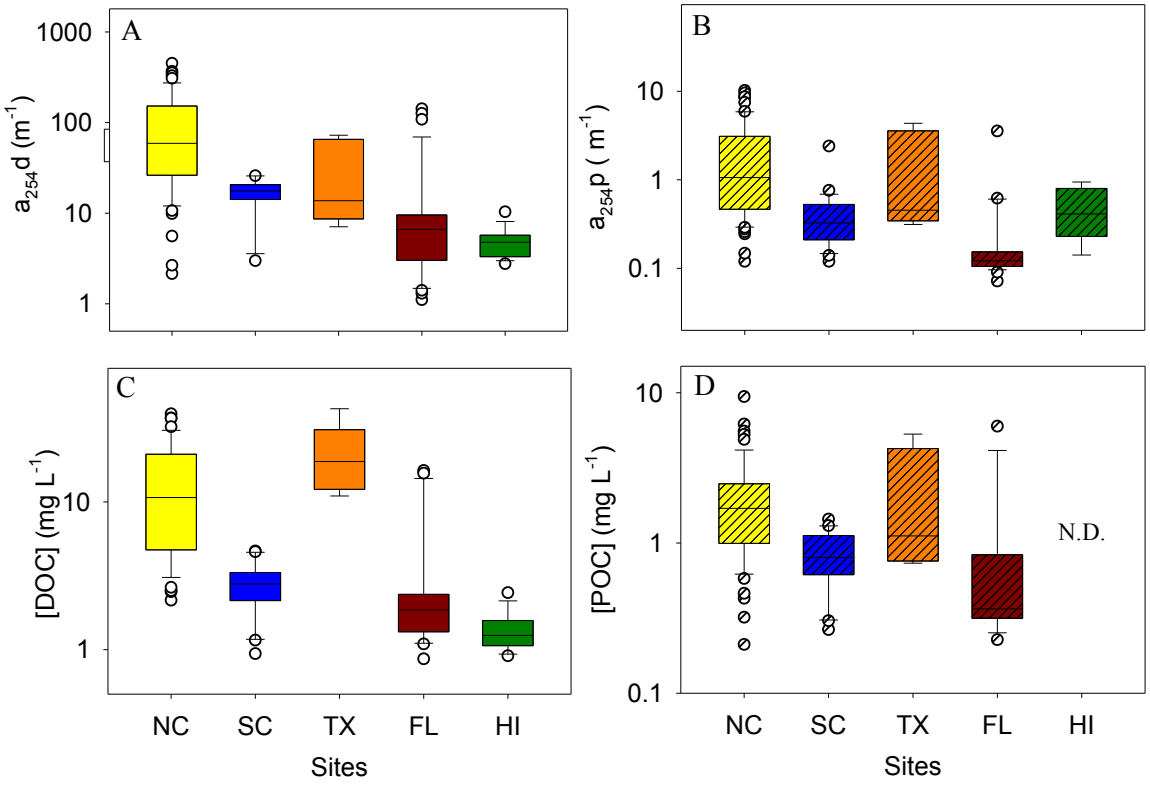

Figure 1. Boxplots summarizing concentration measurements at all five sites. (A-B) a_{254} for CDOM and BEPOM, (C-D) [DOC] and [POC]. Slashes indicate POM. Boxes denote the 10th to the 90th percentiles, the whiskers denote the 5th to the 95th percentiles, and the white circles represent outliers. 'N.D.' indicates no data. Panels A-D were plotted on a log scale.

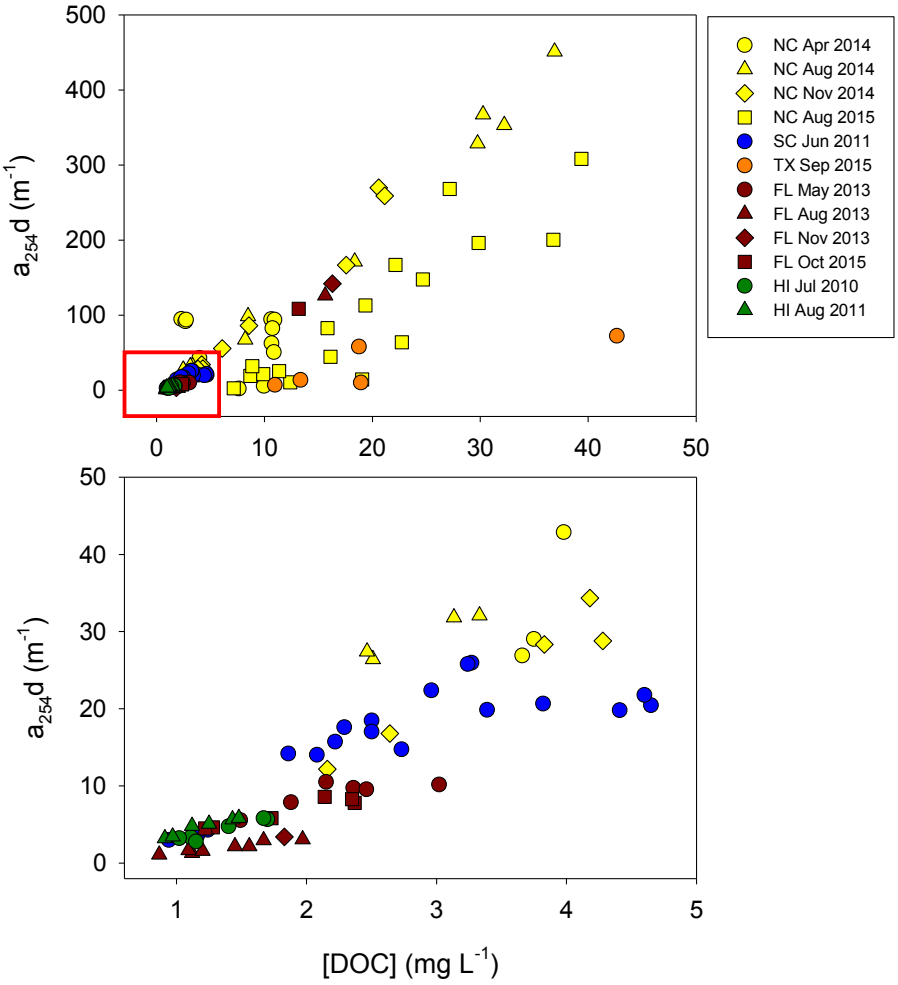

Figure 2. Absorbance at 254 nm ($a_{254}d$) plotted against (A) entire [DOC] and (B) red box enlarged to show smaller concentrations. Sampling locations separated by sampling date.

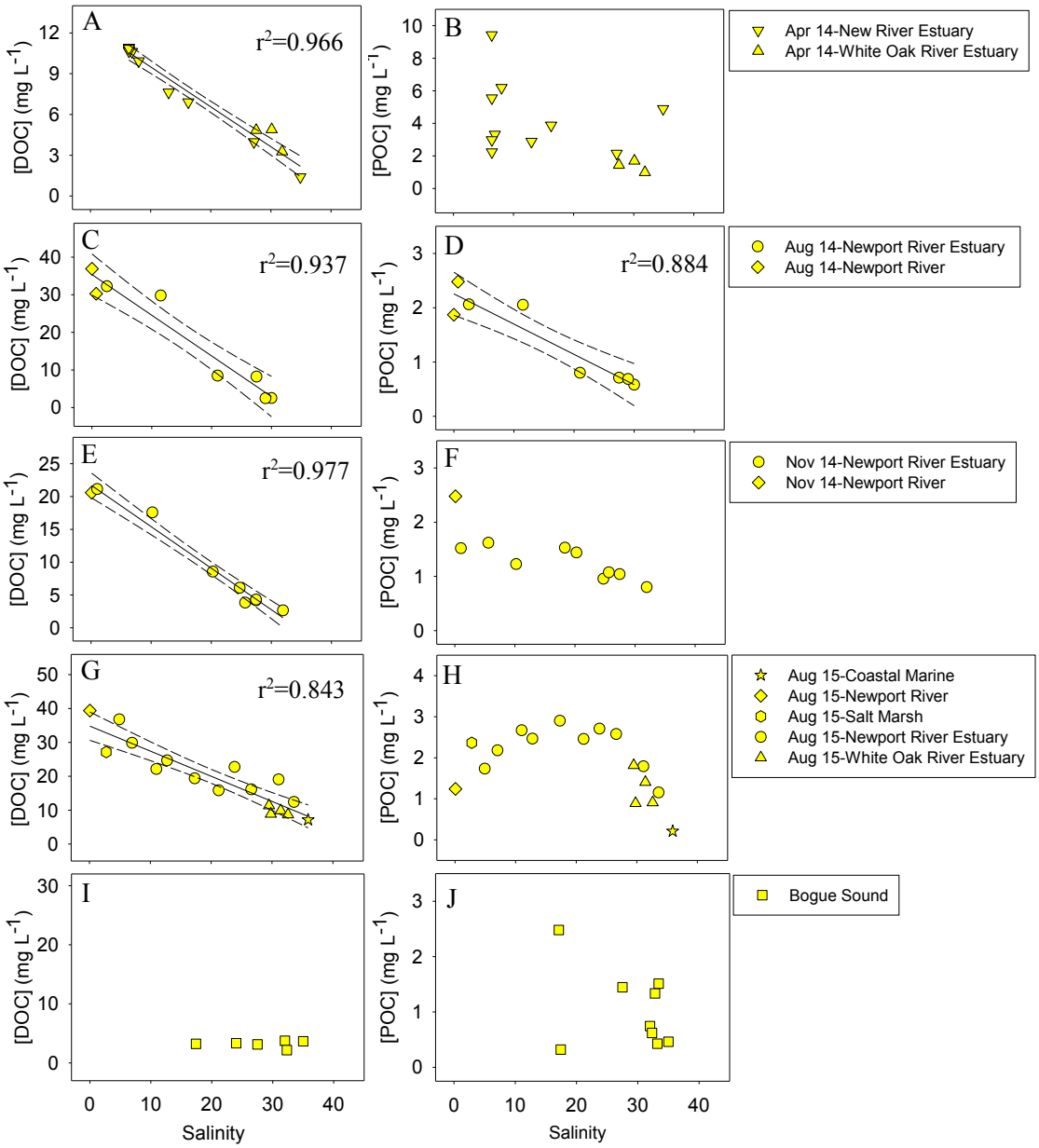

Figure 3. Trends in [DOC] an [POC] with salinity for NC coastal waters during (A-B) April 2014, (C-D) August 2014, (E-F) November 2014, (G-H) August 2015, and (I-J) all sampling dates for Bogue Sound in 2014 and 2015. Linear regressions to the 95% confidence interval are displayed using solid and dashed lines, respectively, and describe the mixing state of the coastal waters. Correlation coefficient (r^2) values were reported if p values for linear regressions were <0.05.

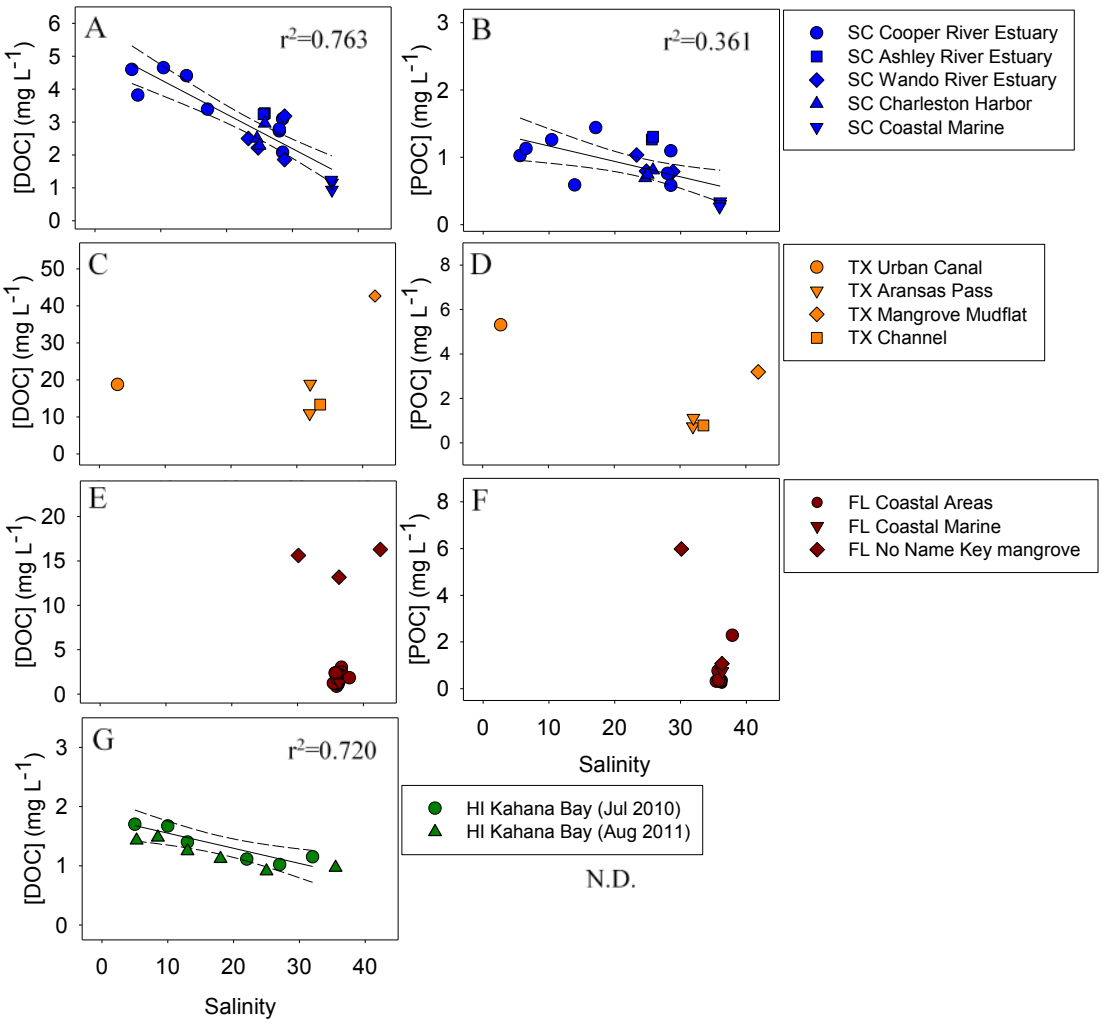

Figure 4. Trends in [DOC] and [POC] versus salinity for (A-B) SC, (C-D), TX, (E-F) FL, and (G) HI coastal waters. 'N.D.' indicates no data. Linear regressions to the 95% confidence interval are displayed using solid and dashed lines, respectively, and describe the mixing state of the coastal waters. Correlation coefficient (r^2) values were reported if p values for the linear regressions were <0.05.

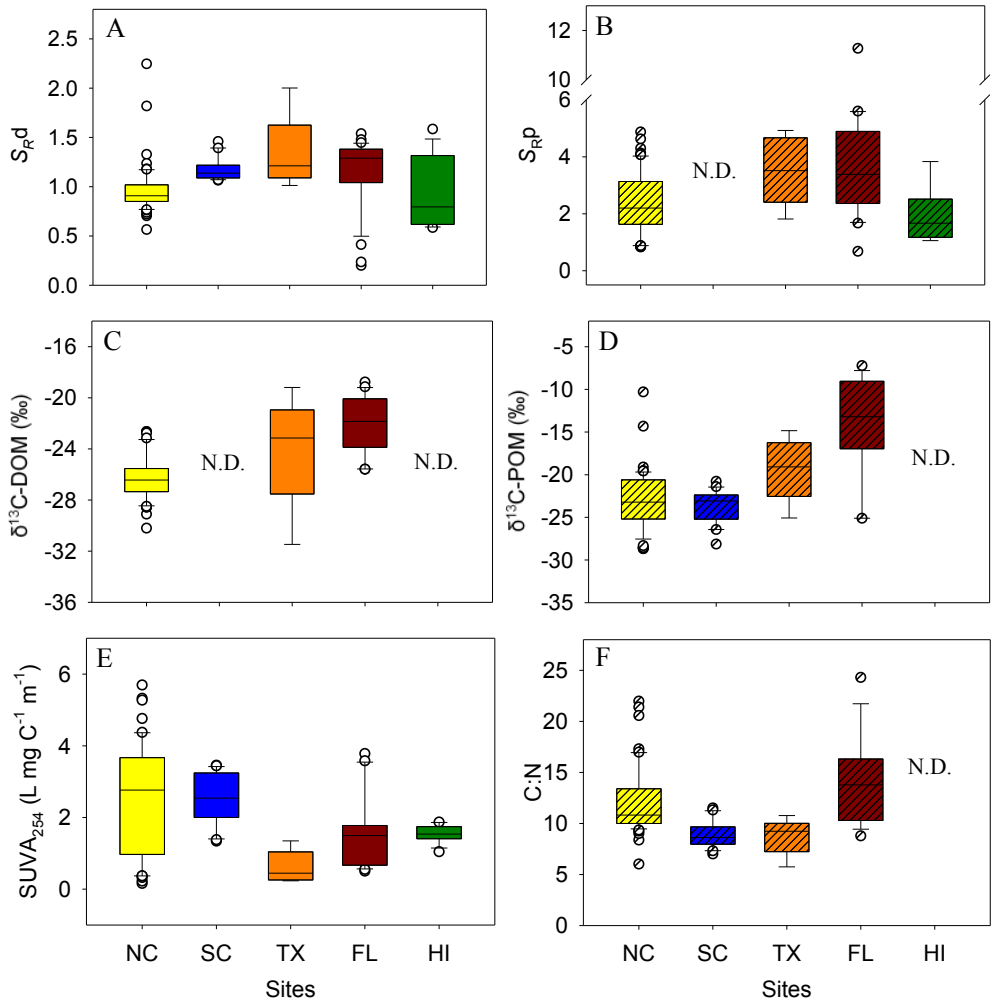

Figure 5. Boxplots of (A-B) CDOM and BEPOM S_R values, (C-D) δ^{13}C-DOM and δ^{13}C-POM, (E) CDOM $SUVA_{254}$, and (F) POM C:N ratios. Slashes indicate POM, and 'N.D.' indicates no data.

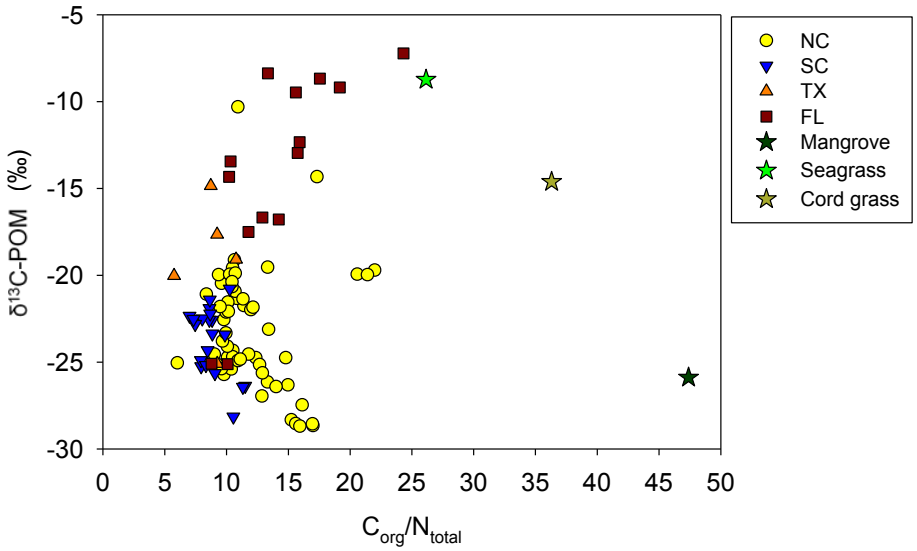

Figure 6. Stable carbon isotopes for POM (δ^{13}C-POM) plotted against molar organic C to total N ratios (C_{org}/N_{total}). No data were available for HI. Stars denote endmember materials such as leaves from red mangrove (*Rhizophora mangle*), turtle sea grass (*Thalassia testudinum*), and cord grass (*Spartina alterniflora).*

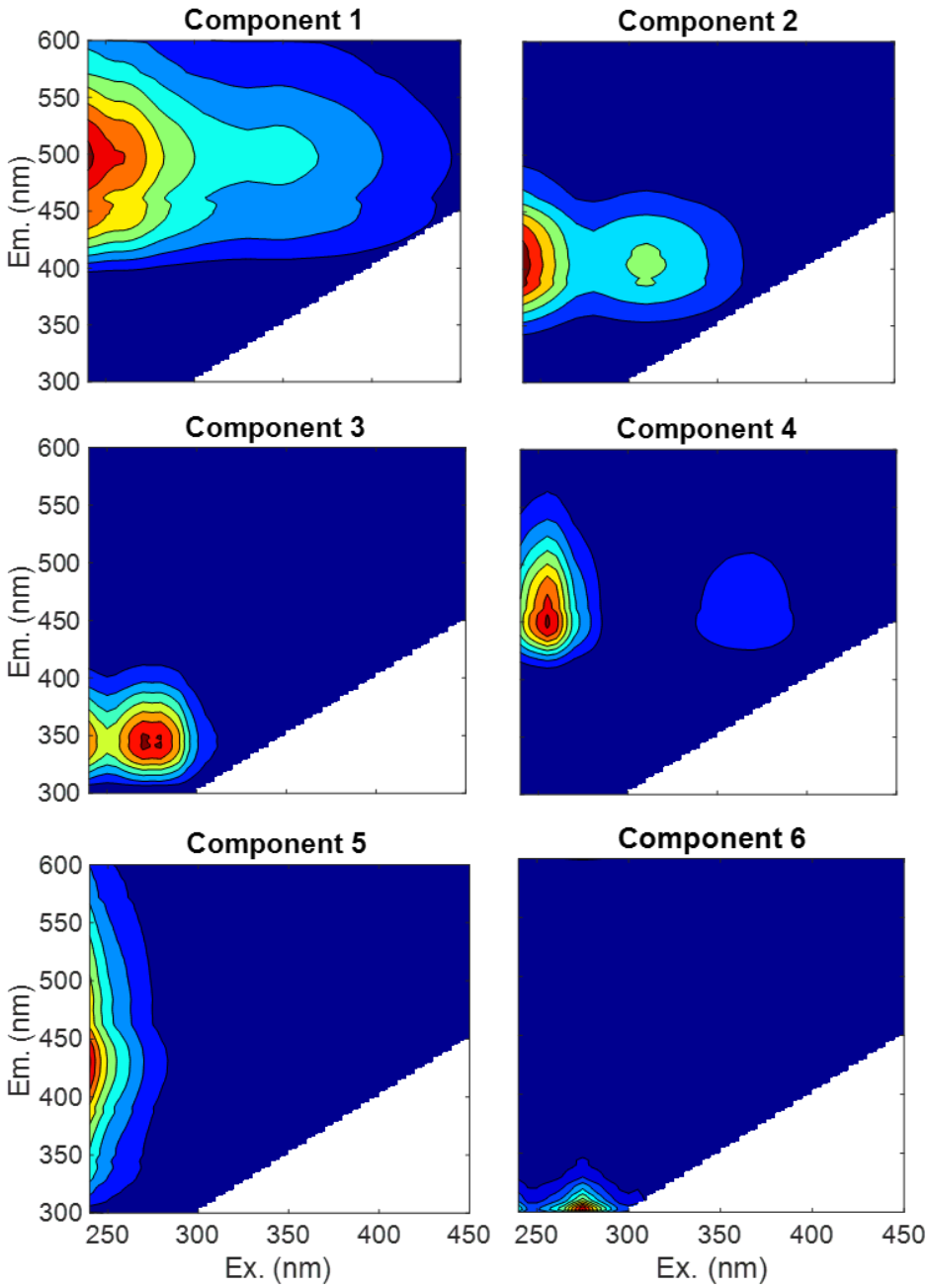

Figure 7. Validated 6-component PARAFAC Model 1 fit to all CDOM and BEPOM EEMs.

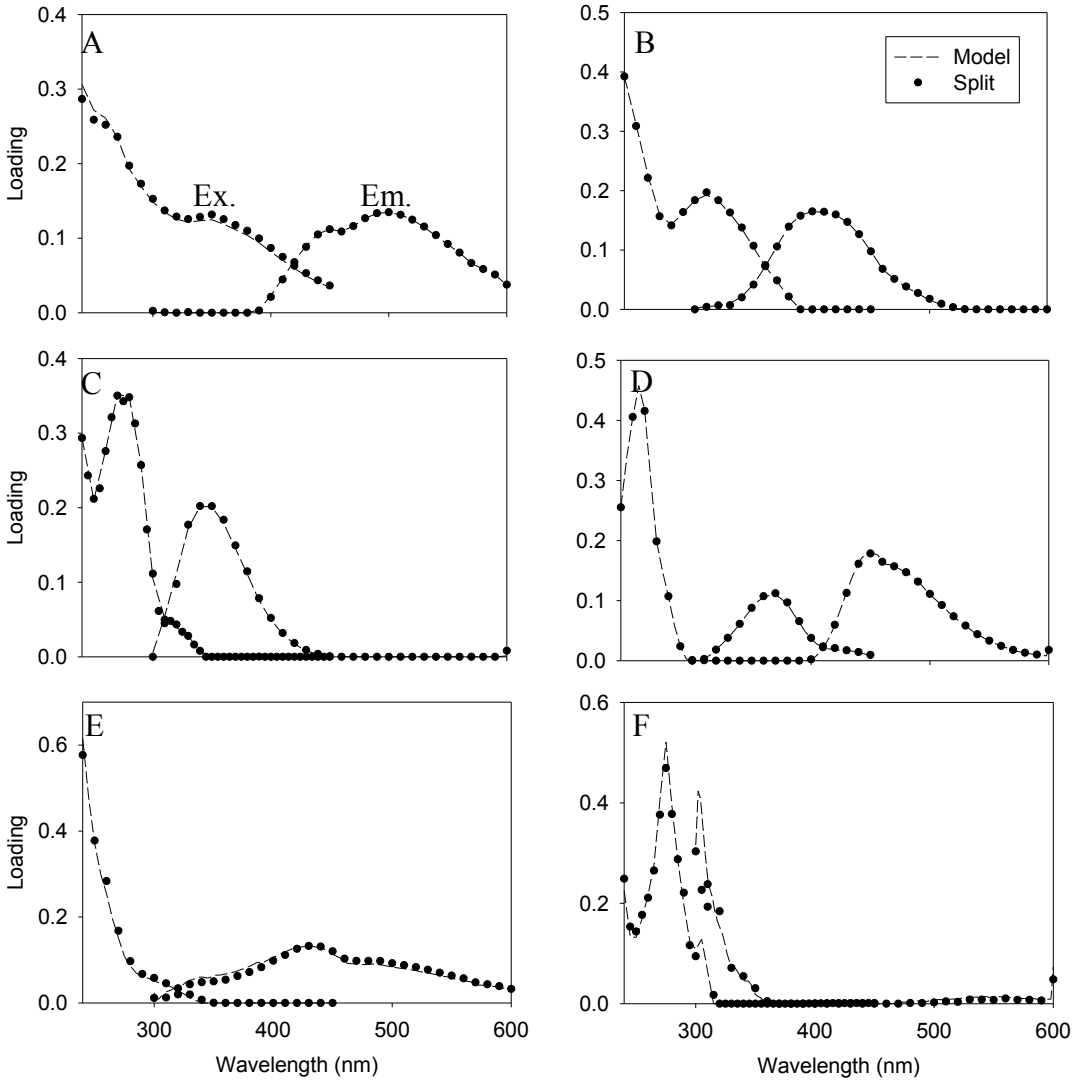

Figure 8. Model 1 excitation ('Ex.') and emission ('Em.') wavelength loadings and split-half validation results. Panels A-F represent C1-C6, respectively.

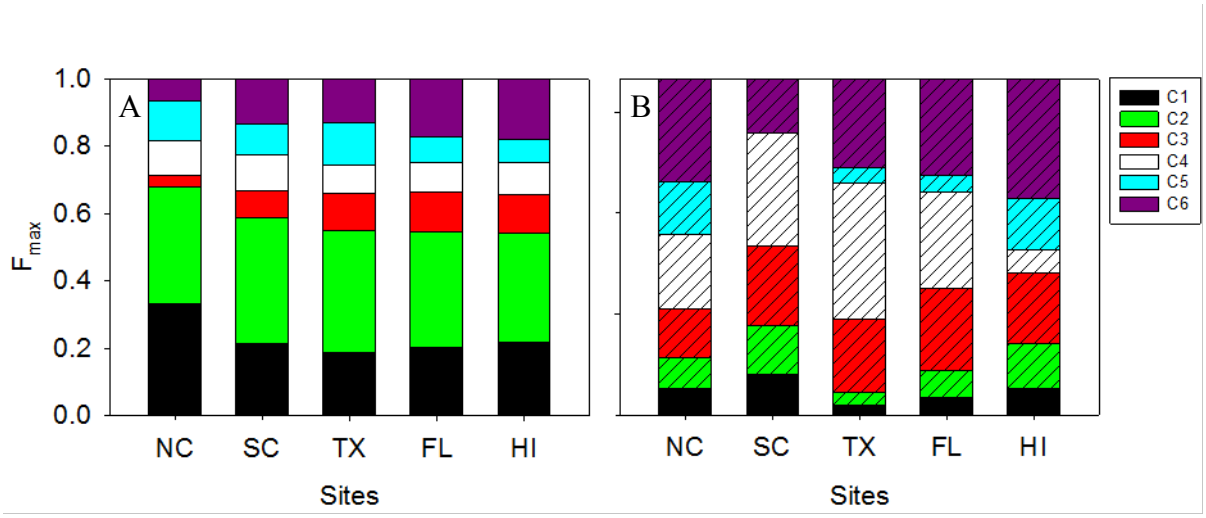

Figure 9. The distribution of fluorescence components from PARAFAC Model 1 in (A) CDOM, and (B) BEPOM. $\%F_{max}$ indicates fluorescence maxima values for relative amounts of components at each site. Slashes indicate BEPOM.

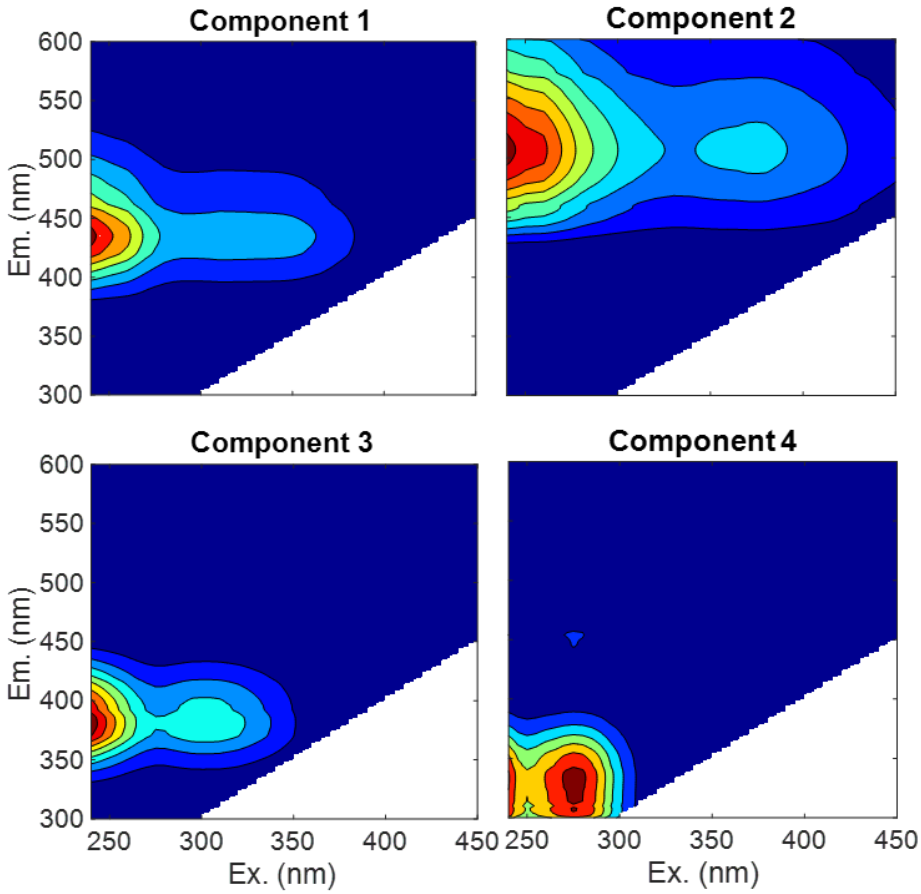

Figure 10. Validated 4-component PARAFAC Model 2 of fluorescent components found in CDOM.

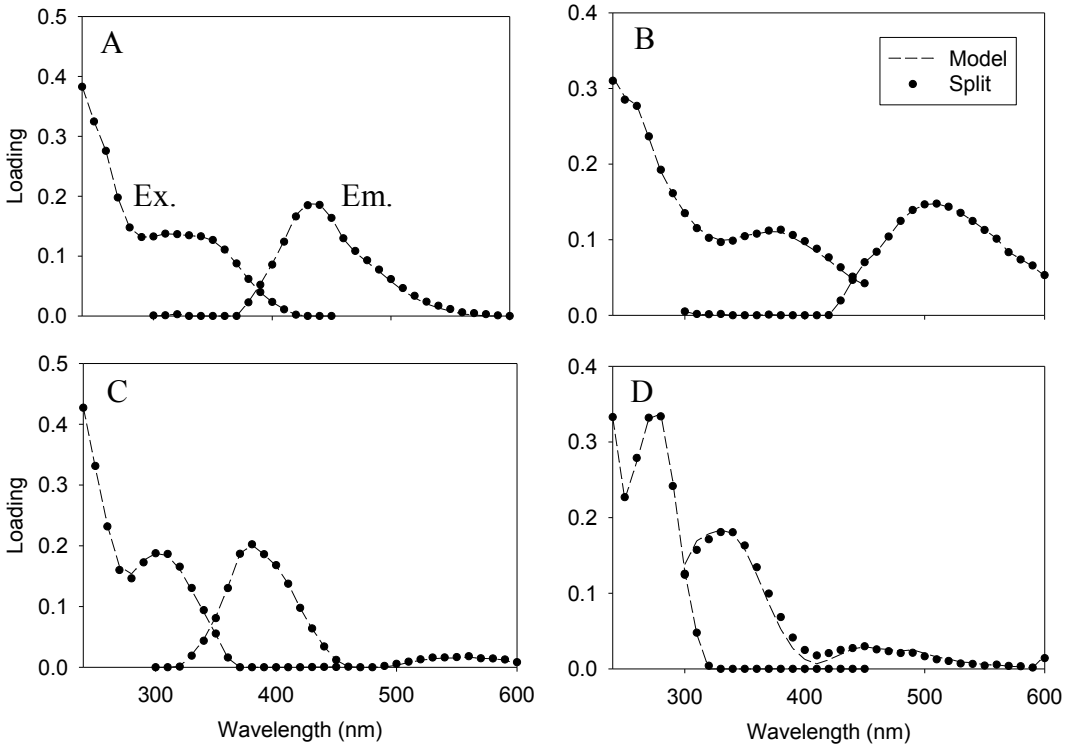

Figure 11. Model 2 excitation ('Ex.') and emission ('Em.') wavelength loadings and split-half validation results. Panels A-D indicate C1-C4, respectively.

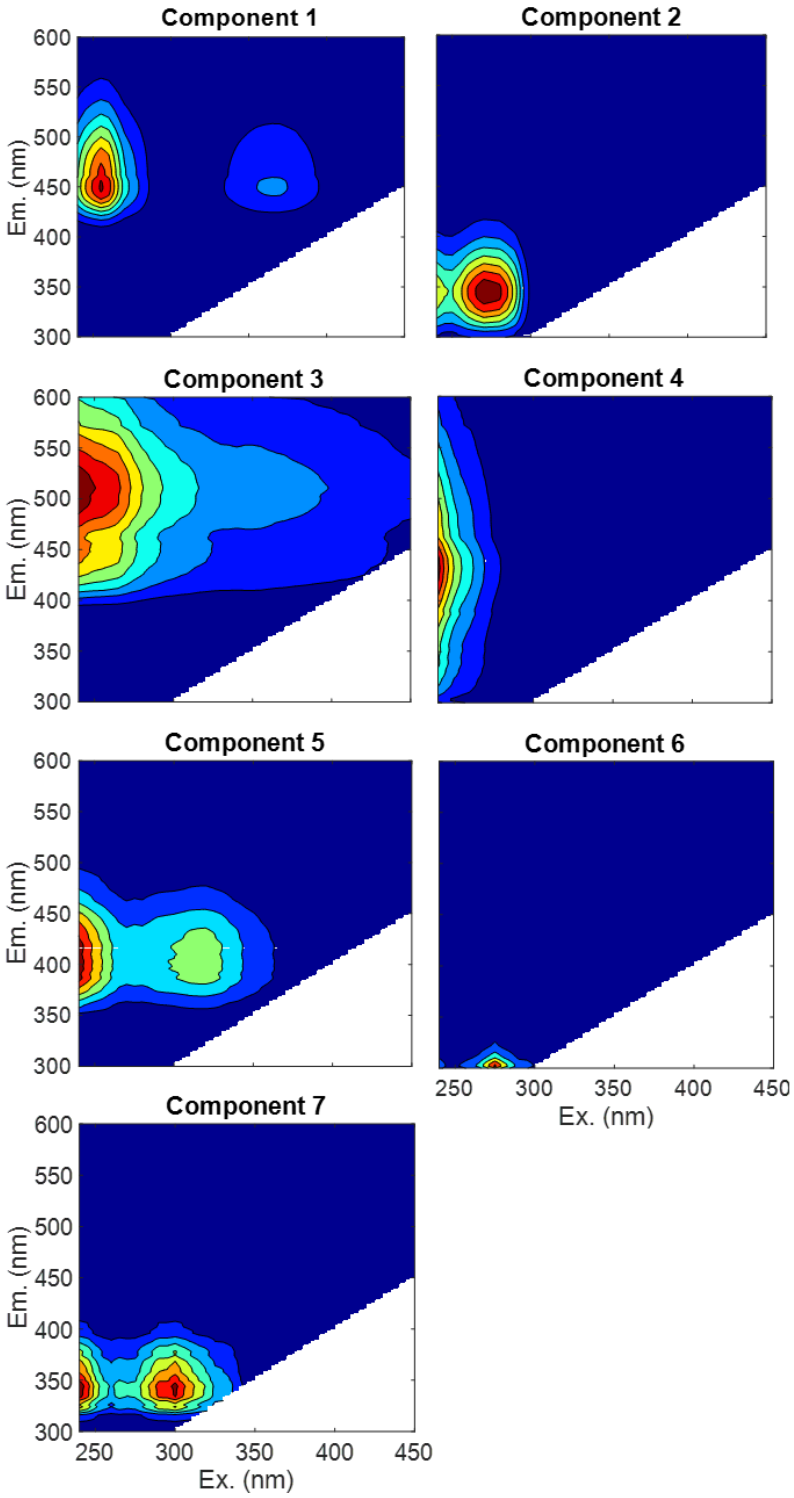

Figure 12. Validated 7-component PARAFAC Model 3 of fluorescent components found in BEPOM.

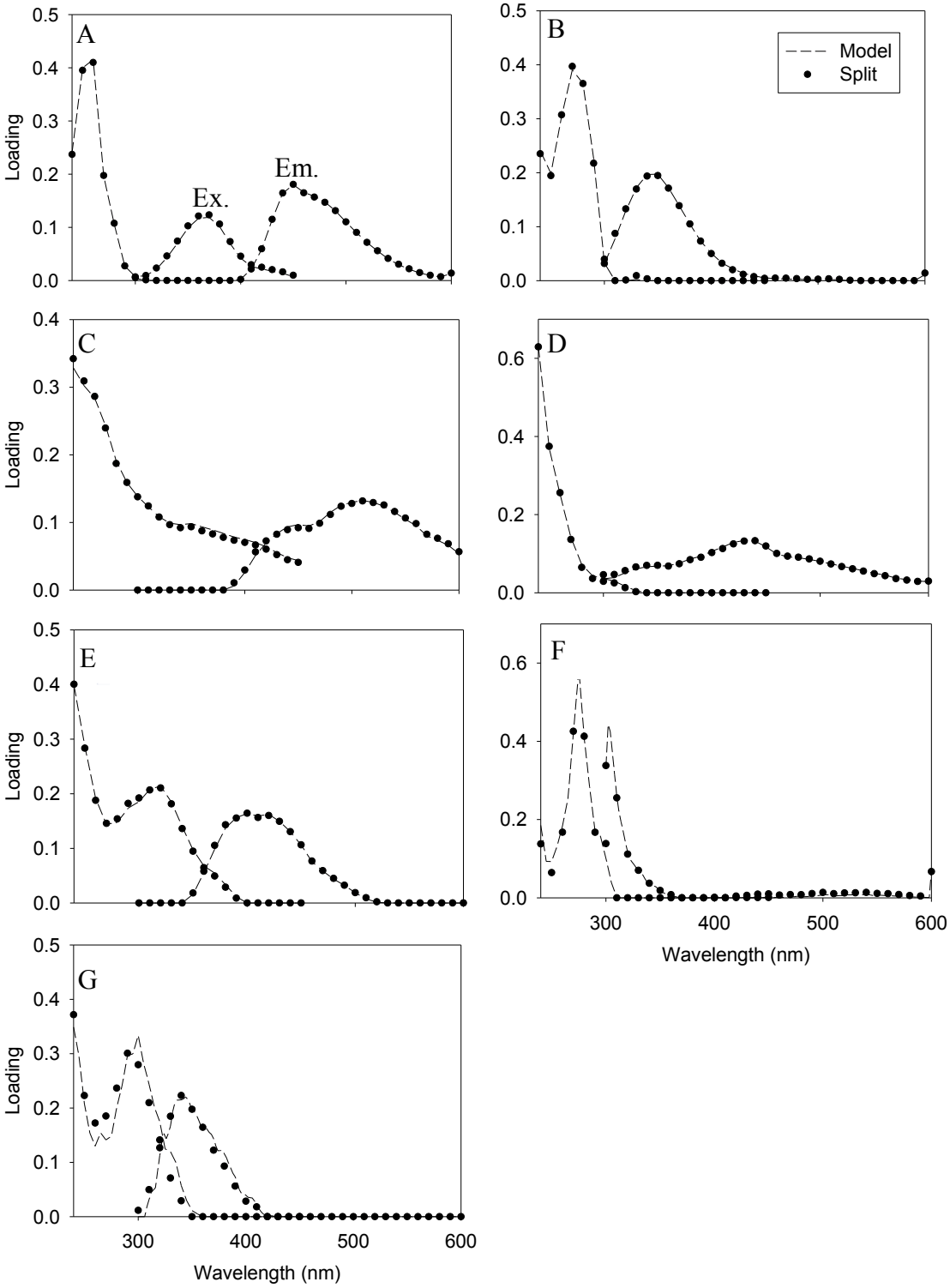

Figure 13. Model 3 excitation ('Ex.') and emission ('Em.') wavelength loadings and split-half validation results. Panels A-G denote C1-C7.

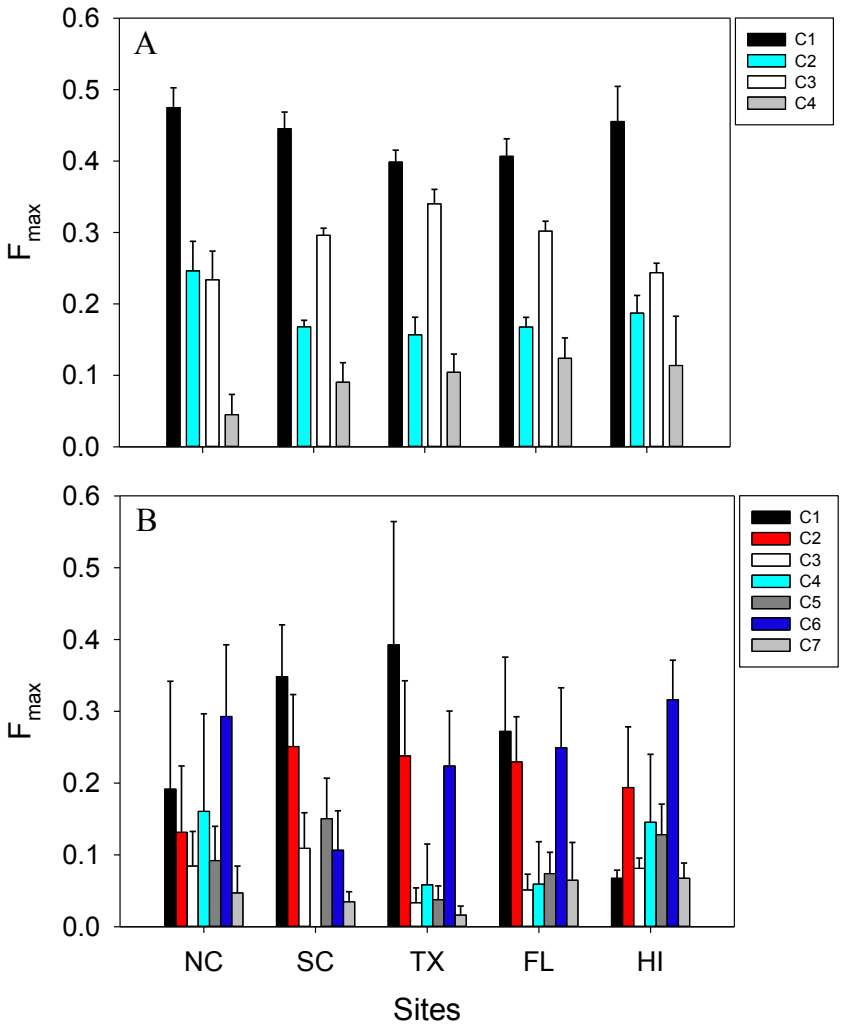

Figure 14. Relative component F_{max} distributions of PARAFAC components from (A) Model 2 and (B) Model 3 at the five sites. Error bars indicate standard deviation.

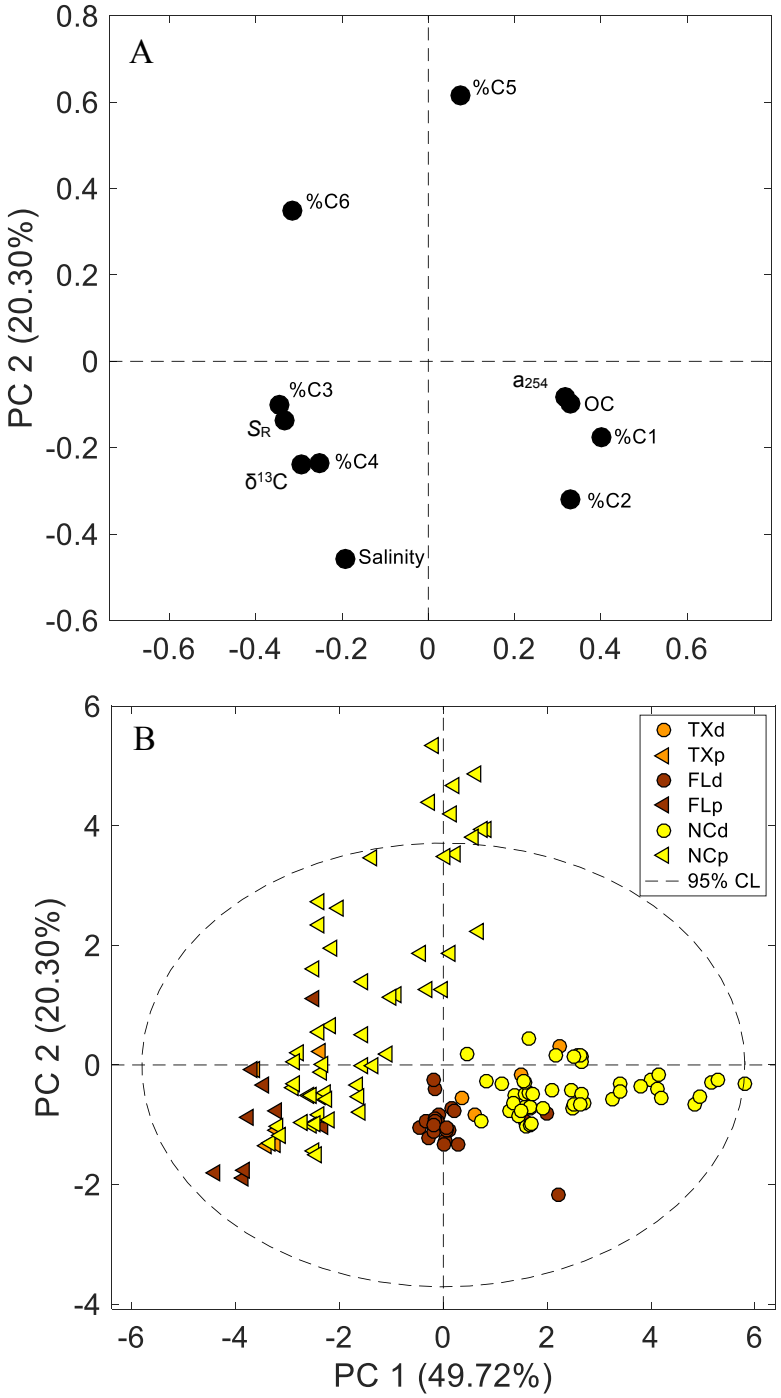

Figure 15. PCA 1 (A) loadings and (B) scores for PARAFAC Model 1 $\%F_{max}$ components, salinity, a_{254}, S_R, OC concentrations, and $\delta^{13}C$ for DOM and POM size fractions. In the legend, 'd' indicates DOM samples while 'p' denotes POM samples. 'CL' stands for confidence level.

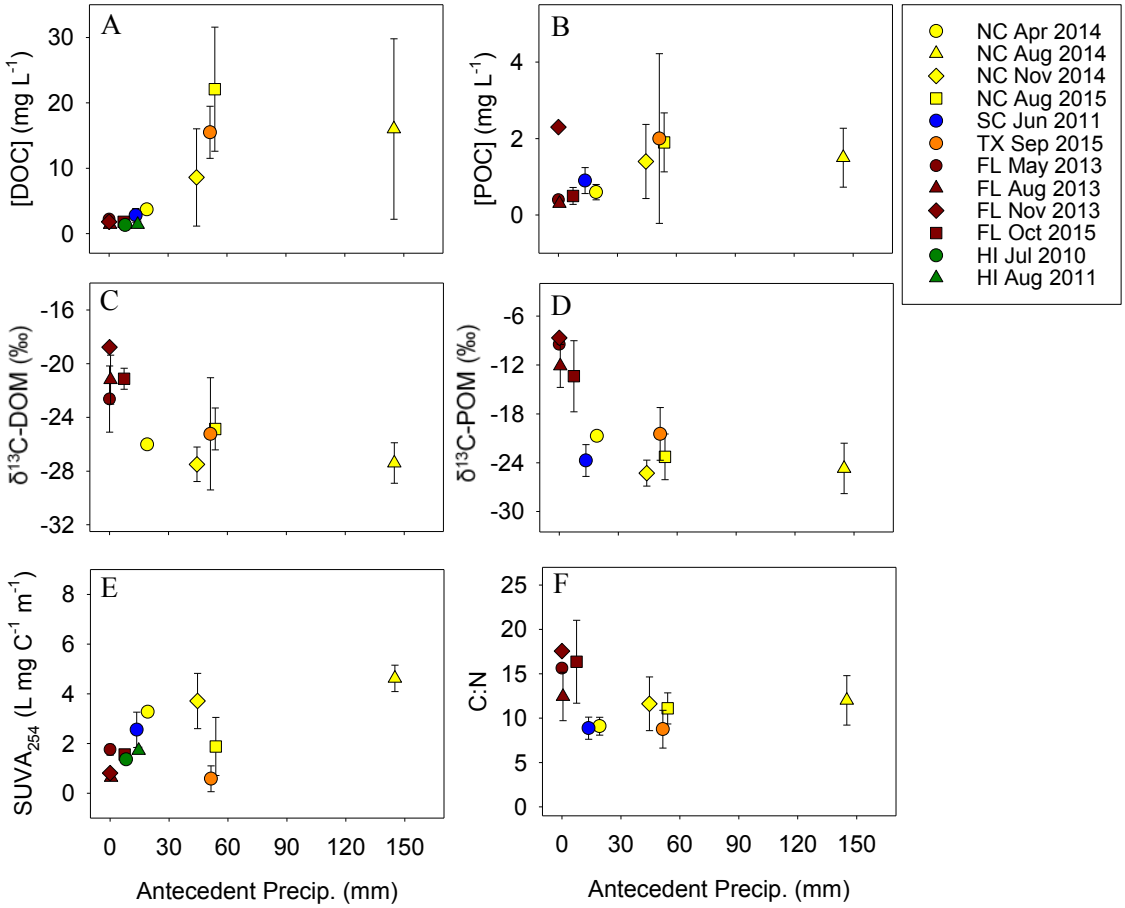

Figure 16. Mean (A-B) [DOC] and [POC], (C-D) δ^{13}C-DOM and δ^{13}C-POM, (E) CDOM $SUVA_{254}$, and (F) POM C:N ratios plotted against antecedent precipitation for seasonal samplings in the five sites. Error bars indicate standard deviation.

REFERENCES

Abril, G., Nogueira, M., Etcheber, H., Cabeçadas, G., Lemaire, E., & Brogueira, M. J. (2002). Behaviour of organic carbon in nine contrasting European estuaries. *Estuarine, Coastal and Shelf Science*, *54*(2), 241-262, doi:10.1006/ecss.2001.0844.

Amaral, V., Graeber, D., Calliari, D., & Alonso, C. (2016). Strong linkages between DOM optical properties and main clades of aquatic bacteria. *Limnology and Oceanography, 61*(3), 906-918, doi:10.1002/lno.10258.

Asmala, E., Autio, R., Kaartokallio, H., Pitkänen, L., Stedmon, C., & Thomas, D. N. (2013). Bioavailability of riverine dissolved organic matter in three Baltic Sea estuaries and the effect of catchment land use. *Biogeosciences*, *10*(11), 6969-6986, doi:10.5194/bg-10-6969-2013.

Benner, R., & Amon, R. M. (2015). The size-reactivity continuum of major bioelements in the ocean. *Annual review of marine science*, *7*, 185-205, doi:10.1146/annurev-marine-010213-135126.

Bauer, J. E., & Bianchi, T. S. (2011). 5.02 Dissolved Organic Carbon Cycling and Transformation. *Treatise on estuarine and coastal science. Academic Press, Waltham*, *5,* 7-67, doi:10.1016/B978-0-12-374711-2.00502-7.

Bauer, J. E., Cai, W. J., Raymond, P. A., Bianchi, T. S., Hopkinson, C. S., & Regnier, P. A. (2013). The changing carbon cycle of the coastal ocean. *Nature*, *504*(7478), 61-70, doi:10.1038/nature12857.

Bianchi, T. S., Pennock, J. R., & Twilley, R. R. (1999). *Biogeochemistry of Gulf of Mexico estuaries*. John Wiley & Sons.

Bianchi, T. S. (2006). *Biogeochemistry of estuaries*. Oxford University Press.

Bianchi, T. S., & Bauer, J. E. (2011). 5.03 Particulate Organic Carbon Cycling and Transformation. *Treatise on Estuarine and Coastal Science. Academic Press, Waltham*, *5,* 69-117, doi:10.1016/B978-0-12-374711-2.00503-9.

Bianchi, T. S., Osburn, C., Shields, M. R., Yvon-Lewis, S., Young, J., Guo, L., & Zhou, Z. (2014). Deepwater Horizon oil in Gulf of Mexico waters after 2 years: Transformation into the dissolved organic matter pool. *Environmental science & technology*, *48*(16), 9288-9297, doi: 10.1021/es501547b.

Bro, R., & Smilde, A. K. (2014). Principal component analysis. *Analytical Methods*, *6*(9), 2812-2831, doi:10.1039/c3ay41907j.

Brym, A., Paerl, H. W., Montgomery, M. T., Handsel, L. T., Ziervogel, K., & Osburn, C. L. (2014). Optical and chemical characterization of base-extracted particulate organic matter in coastal marine environments. *Marine Chemistry*, *162*, 96-113, doi:10.1016/j.marchem.2014.03.006.

Cai, W. J. (2011). Estuarine and coastal ocean carbon paradox: CO2 sinks or sites of terrestrial carbon incineration?. *Annual Review of Marine Science*, *3*, 123-145, doi:10.1146/annurev-marine-120709-142723.

Catalá, T. S., Reche, I., Fuentes-Lema, A., Romera-Castillo, C., Nieto-Cid, M., Ortega-Retuerta, E., Calvo, E., Álvarez, M., Marrasé, C., Stedmon, C. A., & Álvarez-Salgado, X. A. (2015). Turnover time of fluorescent dissolved organic matter in the dark global ocean. *Nature communications*, *6*, doi:10.1038/ncomms6986.

Cawley, K. M., Wolski, P., Mladenov, N., & Jaffé, R. (2012). Dissolved organic matter biogeochemistry along a transect of the Okavango Delta, Botswana. *Wetlands*, *32*(3), 475-486, doi:10.1007/s13157-012-0281-0.

Ciais, P., Sabine, C., Bala, G., Bopp, L., Brovkin, V., Canadell, J., Chhabra, A., DeFries, R., Galloway, J., Heimann, M., Jones, C., Quéré, C. L., Myneni, R. B., Piao, S., & Thornton, P. (2014). Carbon and other biogeochemical cycles. In *Climate change 2013: the physical science basis. Contribution of Working Group I to the Fifth Assessment Report of the Intergovernmental Panel on Climate Change*. Cambridge University Press, 465-570.

Coble, P. G. (1996). Characterization of marine and terrestrial DOM in seawater using excitation-emission matrix spectroscopy. *Marine chemistry*, *51*(4), 325-346, doi:10.1016/0304-4203(95)00062-3.

Coble, P. G. (2007). Marine optical biogeochemistry: the chemistry of ocean color. *Chemical Reviews-Columbus*, *107*(2), 402-418, doi:10.1021/cr050350+.

Coble, P. G., Lead, J., Baker, A., Reynolds, D. M., & Spencer, R. G. (2014). *Aquatic organic matter fluorescence*. Cambridge University Press.

Cole, J. J., Prairie, Y. T., Caraco, N. F., McDowell, W. H., Tranvik, L. J., Striegl, R. G., Duarte, C. M., Kortelainen, P., Downing, J. A., Middleburg, J. J., & Melack, J. (2007). Plumbing the global carbon cycle: integrating inland waters into the terrestrial carbon budget. *Ecosystems*, *10*(1), 172-185, doi:10.1007/s10021-006-9013-8.

Dalzell, B. J., Filley, T. R., & Harbor, J. M. (2007). The role of hydrology in annual organic carbon loads and terrestrial organic matter export from a midwestern agricultural watershed. *Geochimica et Cosmochimica Acta*, *71*(6), 1448-1462, doi:10.1016/j.gca.2006.12.009.

Eimers, M. C., Watmough, S. A., & Buttle, J. M. (2008). Long-term trends in dissolved organic carbon concentration: a cautionary note. *Biogeochemistry*, *87*(1), 71-81, doi:10.1007/s10533-007-9168-1.

Engle, V. D., Kurtz, J. C., Smith, L. M., Chancy, C., & Bourgeois, P. (2007). A classification of US estuaries based on physical and hydrologic attributes. *Environmental Monitoring and Assessment*, *129*(1), 397-412, doi:10.1007/s10661-006-9372-9.

Fellman, J. B., D'Amore, D. V., Hood, E., & Boone, R. D. (2008). Fluorescence characteristics and biodegradability of dissolved organic matter in forest and wetland soils from coastal temperate watersheds in southeast Alaska. *Biogeochemistry*, *88*(2), 169-184, doi:10.1007/s10533-008-9203-x.

Garrison, G. H., Glenn, C. R., & McMurtry, G. M. (2003). Measurement of submarine groundwater discharge in Kahana Bay, O'ahu, Hawaii. *Limnology and Oceanography*, *48*(2), 920-928, doi:10.4319/lo.2003.48.2.0920.

Goñi, M. A., & Thomas, K. A. (2000). Sources and transformations of organic matter in surface soils and sediments from a tidal estuary (North Inlet, South Carolina, USA). *Estuaries*, *23*(4), 548-564, doi:10.2307/1353145.

Hedges, J. I., Keil, R. G., & Benner, R. (1997). What happens to terrestrial organic matter in the ocean?. *Organic geochemistry*, *27*(5), 195-212, doi:10.1016/S0146-6380(97)00066-1.

Hedges, J. I., & Keil, R. G. (1999). Organic geochemical perspectives on estuarine processes: sorption reactions and consequences. *Marine Chemistry*, *65*(1), 55-65, doi:10.1016/S0304-4203(99)00010-9.

Hedges, J. I., Eglinton, G., Hatcher, P. G., Kirchman, D. L., Arnosti, C., Derenne, S., Evershed, R. P., Kögel-Knabner, I., de Leeuw, J. W., Littke, R., Michaelis, W., & Rullkötter, J. (2000). The molecularly-uncharacterized component of nonliving organic matter in natural environments. *Organic geochemistry*, *31*(10), 945-958, doi:10.1016/S0146-6380(00)00096-6.

Helms, J. R., Stubbins, A., Ritchie, J. D., Minor, E. C., Kieber, D. J., & Mopper, K. (2008). Absorption spectral slopes and slope ratios as indicators of molecular weight, source,

and photobleaching of chromophoric dissolved organic matter. *Limnology and Oceanography*, *53*(3), 955-969, doi:10.4319/lo.2008.53.3.0955.

Hood, E., Gooseff, M. N., & Johnson, S. L. (2006). Changes in the character of stream water dissolved organic carbon during flushing in three small watersheds, Oregon. *Journal of Geophysical Research: Biogeosciences*, *111*(G1), doi:10.1029/2005JG000082.

IPCC, 2014: Climate Change 2014: Synthesis Report. Contribution of Working Groups I, II and III to the Fifth Assessment Report of the Intergovernmental Panel on Climate Change [Core Writing Team, R.K. Pachauri and L.A. Meyer (eds.)]. IPCC, Geneva, Switzerland, 151.

Jaffé, R., McKnight, D., Maie, N., Cory, R., McDowell, W. H., & Campbell, J. L. (2008). Spatial and temporal variations in DOM composition in ecosystems: The importance of long-term monitoring of optical properties. *Journal of Geophysical Research: Biogeosciences*, *113*(G4), doi:10.1029/2008JG000683.

Jørgensen, L., Stedmon, C. A., Kragh, T., Markager, S., Middelboe, M., & Søndergaard, M. (2011). Global trends in the fluorescence characteristics and distribution of marine dissolved organic matter. *Marine Chemistry*, *126*(1), 139-148, doi:10.1016/j.marchem.2011.05.002.

Kendall, C., Silva, S. R., & Kelly, V. J. (2001). Carbon and nitrogen isotopic compositions of particulate organic matter in four large river systems across the United States. *Hydrological processes*, *15*(7), 1301-1346, doi:10.1002/hyp.216.

Kirby-Smith, W. W., & Costlow, J. D. (1989). *The Newport River estuarine system*. UNC Sea Grant College Program.

Kottek, M., Grieser, J., Beck, C., Rudolf, B., & Rubel, F. (2006). World map of the Köppen-Geiger climate classification updated. *Meteorologische Zeitschrift*, *15*(3), 259-263, doi:10.1127/0941-2948/2006/0130.

Kowalczuk, P., Durako, M. J., Young, H., Kahn, A. E., Cooper, W. J., & Gonsior, M. (2009). Characterization of dissolved organic matter fluorescence in the South Atlantic Bight with use of PARAFAC model: Interannual variability. *Marine Chemistry*, *113*(3), 182-196, doi:10.1016/j.marchem.2009.01.015.

Kowalczuk, P., Tilstone, G. H., Zabłocka, M., Röttgers, R., & Thomas, R. (2013). Composition of dissolved organic matter along an Atlantic Meridional Transect from fluorescence spectroscopy and Parallel Factor Analysis. *Marine Chemistry*, *157*, 170-184, doi:10.1016/j.marchem.2013.10.004.

Lamb, A. L., Wilson, G. P., & Leng, M. J. (2006). A review of coastal palaeoclimate and relative sea-level reconstructions using δ 13 C and C/N ratios in organic material. *Earth-Science Reviews*, *75*(1), 29-57, doi:10.1016/j.earscirev.2005.10.003.

Lambert, T., Bouillon, S., Darchambeau, F., Massicotte, P., & Borges, A. V. (2016). Shift in the chemical composition of dissolved organic matter in the Congo River network. *Biogeosciences*, *13*(18), 5405, doi:10.5194/bg-13-5405-2016.

Lawaetz, A. J., & Stedmon, C. A. (2009). Fluorescence intensity calibration using the Raman scatter peak of water. *Applied spectroscopy*, *63*(8), 936-940, doi:10.1366/000370209788964548.

Land, L. A., & Paull, C. K. (2001). Thermal gradients as a tool for estimating groundwater advective rates in a coastal estuary: White Oak River, North Carolina, USA. *Journal of Hydrology*, *248*(1), 198-215, doi:10.1016/S0022-1694(01)00405-X.

Lorenzo-Seva, U., & Ten Berge, J. M. (2006). Tucker's congruence coefficient as a meaningful index of factor similarity. *Methodology*, *2*(2), 57-64, doi:10.1027/1614-2241.2.2.57.

Maie, N., Boyer, J. N., Yang, C., & Jaffé, R. (2006). Spatial, geomorphological, and seasonal variability of CDOM in estuaries of the Florida Coastal Everglades. *Hydrobiologia*, *569*(1), 135-150, doi:10.1007/s10750-006-0128-x.

Mannino, A., & Harvey, H. R. (2000). Terrigenous dissolved organic matter along an estuarine gradient and its flux to the coastal ocean. *Organic Geochemistry*, *31*(12), 1611-1625, doi:10.1016/S0146-6380(00)00099-1.

McCallister, S. L., Bauer, J. E., Ducklow, H. W., & Canuel, E. A. (2006). Sources of estuarine dissolved and particulate organic matter: a multi-tracer approach. *Organic Geochemistry*, *37*(4), 454-468, doi:10.1016/j.orggeochem.2005.12.005.

McKee, B. A., Aller, R. C., Allison, M. A., Bianchi, T. S., & Kineke, G. C. (2004). Transport and transformation of dissolved and particulate materials on continental margins influenced by major rivers: benthic boundary layer and seabed processes. *Continental Shelf Research*, *24*(7), 899-926, doi:10.1016/j.csr.2004.02.009.

Mcleod, E., Chmura, G. L., Bouillon, S., Salm, R., Björk, M., Duarte, C. M., Lovelock, C. E., Schlesinger, W. H., & Silliman, B. R. (2011). A blueprint for blue carbon: toward an improved understanding of the role of vegetated coastal habitats in sequestering CO2. *Frontiers in Ecology and the Environment*, *9*(10), 552-560, doi:10.1890/110004.

Mladenov, N., McKnight, D. M., Wolski, P., & Ramberg, L. (2005). Effects of annual flooding on dissolved organic carbon dynamics within a pristine wetland, the Okavango Delta, Botswana. *Wetlands*, *25*(3), 622-638, doi:10.1672/0277-5212(2005)025[0622:EOAFOD]2.0.CO;2.

Moslow, T. F., & Heron Jr, S. D. (1994). The outer banks of North Carolina. In *Geology of Holocene Barrier Island Systems*. Springer Berlin Heidelberg, 47-74, doi:10.1007/978-3-642-78360-9_2.

Murphy, K. R., Ruiz, G. M., Dunsmuir, W. T., & Waite, T. D. (2006). Optimized parameters for fluorescence-based verification of ballast water exchange by ships. *Environmental science & technology*, *40*(7), 2357-2362, doi: 10.1021/es0519381.

Murphy, K. R., Stedmon, C. A., Waite, T. D., & Ruiz, G. M. (2008). Distinguishing between terrestrial and autochthonous organic matter sources in marine environments using fluorescence spectroscopy. *Marine Chemistry*, *108*(1), 40-58, doi:10.1016/j.marchem.2007.10.003.

Murphy, K. R., Hambly, A., Singh, S., Henderson, R. K., Baker, A., Stuetz, R., & Khan, S. J. (2011). Organic matter fluorescence in municipal water recycling schemes: toward a unified PARAFAC model. *Environmental science & technology*, *45*(7), 2909-2916, doi:10.1021/es103015e.

Murphy, K. R., Stedmon, C. A., Graeber, D., & Bro, R. (2013). Fluorescence spectroscopy and multi-way techniques. PARAFAC. *Analytical Methods*, *5*(23), 6557-6566, 10.1039/C3AY41160E.

Murphy K.R., Stedmon C.A., Wenig P., Bro R. (2014). OpenFluor – A spectral database of auto-fluorescence by organic compounds in the environment. *Anal. Methods*, 6, 658-661. doi:10.1039/C3AY41935E.

Nicholls, R. J. (2004). Coastal flooding and wetland loss in the 21st century: changes under the SRES climate and socio-economic scenarios. *Global Environmental Change*, *14*(1), 69-86, doi:10.1016/j.gloenvcha.2003.10.007.

Osburn, C. L., O'Sullivan, D. W., & Boyd, T. J. (2009). Increases in the longwave photobleaching of chromophoric dissolved organic matter in coastal waters. *Limnology and Oceanography*, *54*(1), 145-159, doi:10.4319/lo.2009.54.1.0145.

Osburn, C. L., & Stedmon, C. A. (2011). Linking the chemical and optical properties of dissolved organic matter in the Baltic–North Sea transition zone to differentiate three

allochthonous inputs. *Marine chemistry*, *126*(1), 281-294, doi:10.1016/j.marchem.2011.06.007.

Osburn, C. L., Wigdahl, C. R., Fritz, S. C., & Saros, J. E. (2011). Dissolved organic matter composition and photoreactivity in prairie lakes of the US Great Plains. *Limnology and Oceanography*, *56*(6), 2371-2390, doi:10.4319/lo.2011.56.6.2371.

Osburn, C. L., Handsel, L. T., Mikan, M. P., Paerl, H. W., & Montgomery, M. T. (2012). Fluorescence tracking of dissolved and particulate organic matter quality in a river-dominated estuary. *Environmental science & technology*, *46*(16), 8628-8636, doi:10.1021/es3007723.

Osburn, C. L., Mikan, M. P., Etheridge, J. R., Burchell, M. R., & Birgand, F. (2015). Seasonal variation in the quality of dissolved and particulate organic matter exchanged between a salt marsh and its adjacent estuary. *Journal of Geophysical Research: Biogeosciences*, *120*(7), 1430-1449, doi:10.1002/2014JG002897.

Osburn, C. L., Boyd, T. J., Montgomery, M. T., Bianchi, T. S., Coffin, R. B., & Paerl, H. W. (2016). Optical proxies for terrestrial dissolved organic matter in estuaries and coastal waters. *Frontiers in Marine Science*, *2*, 127, doi:10.3389/fmars.2015.00127.

Peterson, B., Fry, B., Hullar, M., Saupe, S., & Wright, R. (1994). The distribution and stable carbon isotopic composition of dissolved organic carbon in estuaries. *Estuaries and Coasts*, *17*(1), 111-121, doi:10.2307/1352560.

Repeta, D. J. (2014). Chemical characterization and cycling of dissolved organic matter. *Biogeochemistry of Dissolved Organic Matter, Elsevier*, 21-63, doi:10.1016/B978-0-12-405940-5.00002-9.

Revsbæk, M., Mølhave, T., Arge, L., Agarwal, P.K. (2014). ScalgoLive Global. *World Hydrosheds*. Retrieved from http://scalgo.com/live/global.

Reyna, N. E., Hardison, A., & Liu, Z. (2017). Influence of major storm events on the quantity and composition of particulate organic matter and the phytoplankton community in a subtropical estuary, Texas. *Frontiers in Marine Science*, *4*, 43, doi:10.3389/fmars.2017.00043.

Senesi, N. (1990). Molecular and quantitative aspects of the chemistry of fulvic acid and its interactions with metal ions and organic chemicals: Part II. The fluorescence spectroscopy approach. *Analytica Chimica Acta*, *232*, 77-106, doi:10.1016/S0003-2670(00)81225-8.

Shutova, Y., Baker, A., Bridgeman, J., & Henderson, R. K. (2014). Spectroscopic characterisation of dissolved organic matter changes in drinking water treatment: from PARAFAC analysis to online monitoring wavelengths. *Water research*, *54*, 159-169, doi:10.1016/j.watres.2014.01.053.

Solis, R. S., & Powell, G. L. (1999). Hydrography, mixing characteristics, and residence times of Gulf of Mexico estuaries. *Biogeochemistry of Gulf of Mexico estuaries*, 29-61.

Spencer, R. G., Pellerin, B. A., Bergamaschi, B. A., Downing, B. D., Kraus, T. E., Smart, D. R., Dahlgren, R. A., & Hernes, P. J. (2007). Diurnal variability in riverine dissolved organic matter composition determined by in situ optical measurement in the San Joaquin River (California, USA). *Hydrological Processes*, *21*(23), 3181-3189, doi:10.1002/hyp.6887.

Spencer, R. G., Stubbins, A., Hernes, P. J., Baker, A., Mopper, K., Aufdenkampe, A. K., Dyda, R. Y., Mwamba, V. L., Mangangu, A. M., Wabakanghanzi, J. N., & Six, J. (2009). Photochemical degradation of dissolved organic matter and dissolved lignin phenols from the Congo River. *Journal of Geophysical Research: Biogeosciences*, *114*(G3), doi:10.1029/2009JG000968.

Spencer, R. G., Butler, K. D., & Aiken, G. R. (2012). Dissolved organic carbon and chromophoric dissolved organic matter properties of rivers in the USA. *Journal of Geophysical Research: Biogeosciences*, *117*(G3), doi:10.1029/2011JG001928.

Stedmon, C. A., & Markager, S. (2005). Resolving the variability in dissolved organic matter fluorescence in a temperate estuary and its catchment using PARAFAC analysis. *Limnology and Oceanography*, *50*(2), 686-697, doi:10.4319/lo.2005.50.2.0686.

Stedmon, C. A., Markager, S., Søndergaard, M., Vang, T., Laubel, A., Borch, N. H., & Windelin, A. (2006). Dissolved organic matter (DOM) export to a temperate estuary: seasonal variations and implications of land use. *Estuaries and Coasts*, *29*(3), 388-400, doi:10.1007/BF02784988.

Stedmon, C. A., Thomas, D. N., Granskog, M., Kaartokallio, H., Papadimitriou, S., & Kuosa, H. (2007). Characteristics of dissolved organic matter in Baltic coastal sea ice: allochthonous or autochthonous origins?. *Environmental science & technology*, *41*(21), 7273-7279, doi:10.1021/es071210f.

Stedmon, C. A., & Bro, R. (2008). Characterizing dissolved organic matter fluorescence with parallel factor analysis: a tutorial. *Limnology and Oceanography: Methods*, *6*(11), 572-579, doi:10.4319/lom.2008.6.572.

Stedmon, C. A., Thomas, D. N., Papadimitriou, S., Granskog, M. A., & Dieckmann, G. S. (2011). Using fluorescence to characterize dissolved organic matter in Antarctic sea ice brines. *Journal of Geophysical Research: Biogeosciences*, *116*(G3), doi:10.1029/2011JG001716.

Stedmon, C., & Nelson, N. B. (2015). The optical properties of DOM in the ocean. In *Biogeochemistry of Marine Dissolved Organic Matter*. Elsevier Science.

Sulzberger, B., & Durisch-Kaiser, E. (2009). Chemical characterization of dissolved organic matter (DOM): a prerequisite for understanding UV-induced changes of DOM absorption properties and bioavailability. *Aquatic Sciences-Research Across Boundaries*, *71*(2), 104-126, doi:10.1007/s00027-008-8082-5.

Tanaka, K., Kuma, K., Hamasaki, K., & Yamashita, Y. (2014). Accumulation of humic-like fluorescent dissolved organic matter in the Japan Sea. *Scientific reports*, *4*, 5292, doi:10.1038/srep05292.

Tedetti, M., & Sempéré, R. (2006). Penetration of ultraviolet radiation in the marine environment. A review. *Photochemistry and Photobiology*, *82*(2), 389-397, doi:10.1562/2005-11-09-IR-733.

Tremblay, L. B., Dittmar, T., Marshall, A. G., Cooper, W. J., & Cooper, W. T. (2007). Molecular characterization of dissolved organic matter in a North Brazilian mangrove porewater and mangrove-fringed estuaries by ultrahigh resolution Fourier transform-ion cyclotron resonance mass spectrometry and excitation/emission spectroscopy. *Marine chemistry*, *105*(1), 15-29, doi:10.1016/j.marchem.2006.12.015.

Tzortziou, M., Neale, P. J., Osburn, C. L., Megonigal, J. P., Maie, N., & Jaffé, R. (2008). Tidal marshes as a source of optically and chemically distinctive colored dissolved organic matter in the Chesapeake Bay. *Limnology and Oceanography*, *53*(1), 148, doi:10.4319/lo.2008.53.1.0148.

Tzortziou, M., Neale, P. J., Megonigal, J. P., Pow, C. L., & Butterworth, M. (2011). Spatial gradients in dissolved carbon due to tidal marsh outwelling into a Chesapeake Bay estuary. *Marine Ecology Progress Series*, *426*, 41-56, doi:10.3354/meps09017.

Waiser, M. J., & Robarts, R. D. (2004). Photodegradation of DOC in a shallow prairie wetland: evidence from seasonal changes in DOC optical properties and chemical characteristics. *Biogeochemistry*, *69*(2), 263-284, doi:10.0123/B:BIOG.0000031048.20050.4e.

Walker, S. A., Amon, R. M., Stedmon, C., Duan, S., & Louchouarn, P. (2009). The use of PARAFAC modeling to trace terrestrial dissolved organic matter and fingerprint

water masses in coastal Canadian Arctic surface waters. *Journal of Geophysical Research: Biogeosciences*, *114*(G4), doi:10.1029/2009JG000990.

Weishaar, J. L., Aiken, G. R., Bergamaschi, B. A., Fram, M. S., Fujii, R., & Mopper, K. (2003). Evaluation of specific ultraviolet absorbance as an indicator of the chemical composition and reactivity of dissolved organic carbon. *Environmental science & technology*, *37*(20), 4702-4708, doi: 10.1021/es030360x.

Williams, C. J., Yamashita, Y., Wilson, H. F., Jaffé, R., & Xenopoulos, M. A. (2010). Unraveling the role of land use and microbial activity in shaping dissolved organic matter characteristics in stream ecosystems. *Limnology and Oceanography*, *55*(3), 1159, doi:10.4319/lo.2010.55.3.1159.

Ya, C., Anderson, W., & Jaffé, R. (2015). Assessing dissolved organic matter dynamics and source strengths in a subtropical estuary: application of stable carbon isotopes and optical properties. *Continental Shelf Research*, *92*, 98-107, doi:10.1016/j.csr.2014.10.005.

Yamashita, Y., Jaffé, R., Maie, N., & Tanoue, E. (2008). Assessing the dynamics of dissolved organic matter (DOM) in coastal environments by excitation emission matrix fluorescence and parallel factor analysis (EEM-PARAFAC). *Limnology and Oceanography*, *53*(5), 1900-1908, doi:10.4319/lo.2008.53.5.1900.

Yamashita, Y., Scinto, L. J., Maie, N., & Jaffé, R. (2010). Dissolved organic matter characteristics across a subtropical wetland's landscape: application of optical properties in the assessment of environmental dynamics. *Ecosystems*, *13*(7), 1006-1019, doi:10.1007/s10021-010-9370-1.

Yamashita, Y., Nosaka, Y., Suzuki, K., Ogawa, H., Takahashi, K., & Saito, H. (2013). Photobleaching as a factor controlling spectral characteristics of chromophoric dissolved organic matter in open ocean. *Biogeosciences*, *10*(11), 7207-7217, doi:10.5194/bg-10-7207-2013.

Zhang, Y., van Dijk, M. A., Liu, M., Zhu, G., & Qin, B. (2009). The contribution of phytoplankton degradation to chromophoric dissolved organic matter (CDOM) in eutrophic shallow lakes: field and experimental evidence. *water research*, *43*(18), 4685-4697, doi:10.1016/j.watres.2009.07.024.